



HAL
open science

Recent advances on Naphthoquinone-imidazolyl and Naphthoquinone-thiazolyl derivatives as photoinitiators of photopolymerization

Frédéric Dumur

► **To cite this version:**

Frédéric Dumur. Recent advances on Naphthoquinone-imidazolyl and Naphthoquinone-thiazolyl derivatives as photoinitiators of photopolymerization. *European Polymer Journal*, 2024, 219, pp.113401. 10.1016/j.eurpolymj.2024.113401 . hal-04681505

HAL Id: hal-04681505

<https://hal.science/hal-04681505v1>

Submitted on 29 Aug 2024

HAL is a multi-disciplinary open access archive for the deposit and dissemination of scientific research documents, whether they are published or not. The documents may come from teaching and research institutions in France or abroad, or from public or private research centers.

L'archive ouverte pluridisciplinaire **HAL**, est destinée au dépôt et à la diffusion de documents scientifiques de niveau recherche, publiés ou non, émanant des établissements d'enseignement et de recherche français ou étrangers, des laboratoires publics ou privés.

Recent advances on Naphthoquinone-imidazolyl and Naphthoquinone-thiazolyl derivatives as photoinitiators of photopolymerization

Frédéric Dumur^{a*}

^a Aix Marseille Univ, CNRS, ICR, UMR 7273, F-13397 Marseille, France

frederic.dumur@univ-amu.fr

Abstract

Visible light photopolymerization is facing a revolution with the development of energy-efficient light sources, namely LEDs. With the ongoing efforts to develop photoinitiating systems outperforming the existing ones in terms of polymerization rates and monomer conversions, the search for new families of dyes that have not been investigated yet in the context of photopolymerization is still very active from the academic viewpoint. Recently, naphthoquinone-imidazolyl and naphthoquinone-thiazole derivatives have been identified as interesting structures for designing both Type I and Type II photoinitiators activable under artificial light sources or Sun. Naphthoquinones are biosourced compounds that can greatly reduce the carbon footprint of photopolymerization. Naphthoquinones are also cheap precursors for the design of photoinitiators, enabling to design low-cost light absorbing structures. By their broad absorption spectra, naphthoquinones are also excellent candidates for the design of sunlight photoinitiators. In this review, the different structures developed with these two scaffolds are reported and comparisons of photoinitiating abilities are presented.

Keywords

Photopolymerization; naphthoquinone; thiazole; imidazole; Sunlight-induced polymerization

1. Introduction

Photopolymerization is a popular polymerization technique nowadays used in applications such as dentistry, adhesives, microelectronics or coatings.[1–12] Its scope of applications has been greatly expanded in recent years thanks to the development of inexpensive and energy-efficient light sources emitting in the visible range, namely LEDs.[13–20] Indeed, for decades, UV photopolymerization has been predominant but the high cost of the irradiation setups, the elevated energy consumption,[21–26] as well as the safety concerns raised by the use of UV light have irremediably discarded UV photopolymerization in favour of visible light photopolymerization. [27–36] Use of visible light is not only beneficial in terms of safety for the manipulator but also for the depth of cure. Indeed, if the light penetration in the UV range is limited to a few hundreds of micrometers, this value can increase up to a few centimeters in the near infrared range.[37] Parallel to this first advantage, other benefits such

as a temporal and a spatial control can also be mentioned, making photopolymerization an interesting polymerization technique for numerous applications. However, a spatial and a temporal control is only required for applications such as 3D-printing and dentistry. In the case of adhesives or paints used in outdoor applications, such a control is totally useless, evidencing the broadness of applications of visible light photopolymerization. By optimizing the design of photoinitiators, excellent monomer conversions can nowadays be obtained under sunlight, paving the way for costless polymerization processes and outdoor applications.[38–44] Besides, compared to photoinitiators that are activated with artificial light sources and for which the excitation wavelength can be selected in order to perfectly fit the absorption spectra of photoinitiators and the light intensity adjusted in order to improve the reactivity of the photoinitiating systems, such an adaptation of the reaction conditions is not possible with sunlight. The development of sunlight photoinitiators is thus more difficult than LED-activated photoinitiators. Notably, the low light intensity of Sun (around 5 mW/cm²), and the broadness of its absorption spectrum can be cited as the two main parameters rendering the development of sunlight photoinitiators challenging. At present, most of sunlight photoinitiators still lack of reactivity, and comparisons of the polymerization kinetics obtained with LEDs and sunlight are still disfavorable for sunlight experiments.[2,44–48] Face to these considerations, the development of sunlight photoinitiators could only be achieved by screening a wide range of structures. Considering that the chemical modification of UV photoinitiators was a hard task to redshift their absorptions towards the visible range and that the basic scaffold of these structures was not adapted for elaborating dyes with extremely broad absorption spectra, structures totally disconnected from these historical UV photoinitiators had to be developed. Among the most popular scaffolds investigated in the literature for the design of visible light photoinitiators, carbazole,[49–52] pyrenes,[53–55] naphthalimides,[56,57] iridium complexes,[58,59] copper complexes,[60–64] iron complexes,[65–67] cyanines,[68–72] chalcones,[73–77] or truxene derivatives,[78] have been examined for designing dyes enabling to polymerize at different irradiation wavelengths. In some cases, panchromatic photoinitiators that can be indifferently excited at different irradiation wavelengths while maintaining an excellent polymerization efficiency have even been reported in the literature.[79–90] Nowadays, another topic of interest concerns the design of biosourced photoinitiators, enabling to reduce the carbon footprint of photoinitiators. Notably, chromones and flavones,[91–93] camphorquinones,[94,95] curcumin,[96–99] chlorophyll,[100,101] vanillin,[102,103] β -carotene,[104–107] riboflavin (vitamin B₂),[108–121] or paprika[122] have been examined for this purpose. Among biosourced compounds, the family of naphthoquinones is another source of biosourced photoinitiators and derivatives such as vitamins K₁ and K₃ proved to be efficient photoinitiators activable at 405 nm.[123–131] Two naturally derived naphthoquinone derivatives, namely 5-hydroxy-1,4-naphthoquinone (5HNQ) and 2-hydroxy-1,4-naphthoquinone (2HNQ) could initiate the free radical polymerization (FRP) of acrylates or the cationic polymerization (CP) of epoxides upon excitation at 410 and 455 nm.[128] With aim at redshifting their absorptions towards the visible range, the extension of π -conjugation is an efficient strategy. Notably, the design of 1*H*-naphtho[2,3-*d*]imidazole-4,9-dione (NAP-I)[132–136] and naphtho[2,3-*d*]thiazole-4,9-dione (NAP-T)[137] resulting from the fusion between the naphthoquinone moiety, an imidazole

and a thiazole ring has been reported in the literature (See Figure 1). However, these structures have been investigated for their biological activities[134,135] or for the development of new synthetic methodologies,[133,136] and none of these structures have been examined for their photophysical, electrochemical or optical properties. Concerning the synthesis of NAP-I and NAP-T, the specific synthetic routes developed for preparing these 1,4-naphthoquinone derivatives are unique and cannot be transposed to the synthesis of analogues based on 1,4-benzoquinone. In this case, other synthetic routes have to be used, using 1,4-dimethoxybenzene as the starting materials and not *para*-benzoquinone.[138] To end, no benzoquinone analogues of NAP-T have been reported yet in the literature, evidencing the challenge existing in the synthesis of these structures.

In 2022, the scope of application of 1*H*-naphtho[2,3-*d*]imidazole-4,9-dione (NAP-I) and naphtho[2,3-*d*]thiazole-4,9-dione (NAP-T) has been extended to visible light and sunlight photopolymerization. Notably, the 2-phenyl-1*H*-naphtho[2,3-*d*]imidazole-4,9-dione scaffold was examined in order to design a series of Type I photoinitiators derived from the well-known oxime esters. Following this pioneering work, 2-phenyl-1*H*-naphtho[2,3-*d*]imidazole-4,9-dione and 2-phenylnaphtho[2,3-*d*]thiazole-4,9-dione derivatives have been designed as Type I and Type II photoinitiators, but also as solar photoinitiators. Choice of the naphthoquinone scaffold was notably justified by the strong colour of the precursor (i.e. 1,4-naphthoquinone is a deep brown solid), and the elaboration of dyes that can strongly absorb in the visible range can thus be anticipated. Considering that the investigation of such structures was unprecedented in the literature, their polymerization efficiencies could not be anticipated, deserving thus to be studied. These different structures have been investigated by Lalevée and coworkers who is THE world leader group in the search for photoinitiators of innovative structures disconnected from historical photoinitiators. Interesting results could thus be expected/anticipated with these naphthoquinone derivatives. Considering that the precursor is deep yellow, dyes strongly absorbing at 405 nm can thus be expected, perfectly fitting with the wavelength under use in 3D-printers. The strong expertise of this group is thus once again highlighted. It has to be noticed that, in the different works detailed in this review, only multifunctional monomers have been investigated. Insoluble crosslinked polymers are thus obtained after polymerization. Even if different reaction pathways can be envisioned, the most important feature for crosslinked polymers and thus coatings is to produce tack-free polymers with the shortest irradiation time.

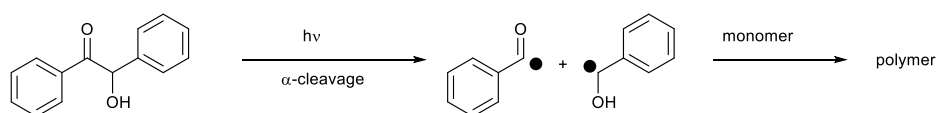


Figure 1. Structures of different naphthoquinone with fused structures (imidazole or thiazole)

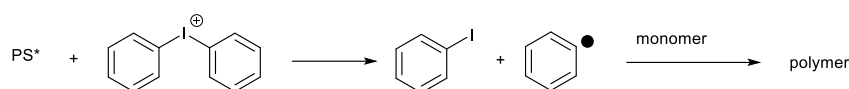
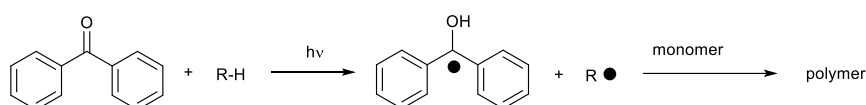
In terms of photoinitiation, two distinct categories of photoinitiators exist. The first one, named Type I photoinitiators are capable to generate radicals by photocleavage of a specific bond introduced in their scaffold. These structures are thus monocomponent systems.

Conversely, Type II photoinitiators can only generate radicals by mean of a hydrogen abstraction mechanism (as observed with benzophenone see Scheme 1), but also by a photoinduced electron transfer towards an electron-deficient onium salt. Even if a few examples of monocomponent systems have notably been reported with benzophenone derivatives,[139,140] sulfonium[141] or iodonium salts,[142–144] Type II photoinitiators are mostly used in two or three-component systems.[145–148]

Type I



Type II



Scheme 1. Radical generation with Type I and Type II photoinitiators.

In this review, the different photoinitiators reported since 2022 as structures activable under artificial light sources and/or sunlight and comprising these two scaffolds are presented. Even if some of these structures only showed moderate photoinitiating abilities, from my viewpoint, the quest for new photoinitiators exhibiting improved photoinitiating abilities at 405 nm and under sunlight should remain the focus of intense research efforts. Considering that these photoinitiators have been investigated in similar conditions, comparisons between phenyl-1*H*-naphtho[2,3-*d*]imidazole-4,9-dione and 2-phenylnaphtho[2,3-*d*]thiazole-4,9-dione derivatives can be established.

2. Derivatives of 2-phenyl-1*H*-naphtho[2,3-*d*]imidazole-4,9-dione

2.1. Type I photoinitiators

Type I photoinitiators are extensively studied both in academy and in industry due to their unique abilities to generate initiating radicals without additives.[13,149–152] These monocomponent systems are numerous in the literature and among the most popular structures, trichloromethyl-*S*-triazine glyoxylates, acyloximino esters, phosphine oxides, hydroxyacetophenones, α -aminoalkylacetophenones, benzoin derivatives, benzylketals, oxime esters, glyoxylates, *o*-acyl- α -oximino ketones, hexaaryl biimidazoles (HABIs) and α -haloacetophenones were reported in the literature.[153] The first report mentioning the use of the 2-phenyl-1*H*-naphtho[2,3-*d*]imidazole-4,9-dione scaffold for the design of Type I photoinitiators was published in 2022.[154] Two series of Type I photoinitiators were prepared, differing by the substitution pattern of the phenyl ring (See Figure 2). As a control product, a non-cleavable compound was synthesized, namely compound 1. Contrarily to Type

II photoinitiators that can only generate initiating species by mean of a two- or a three-component system, Type I photoinitiators can generate radicals by homolytic cleavage of a specific bond introduced in their scaffolds. Among Type I photoinitiators, oxime esters that can homolytically cleave and generate initiating radicals by homolytic cleavage of the N-O bond have been extensively studied during the last three years, these compounds acting as monocomponent photoinitiators.[155–166] Additionally, oxime esters can be prepared in a few steps starting from cheap and easily available reagents, making these structure highly attractive.[167–171] From a mechanistic viewpoint, the advantage of the monocomponent systems are numerous compared to the multicomponent. Indeed, with monocomponent systems, the generation of radical is not dependent of the viscosity of the resin, the efficiency of the photoinduced electron transfer which are key elements governing the ability of the multicomponent photoinitiating systems to generate radicals.

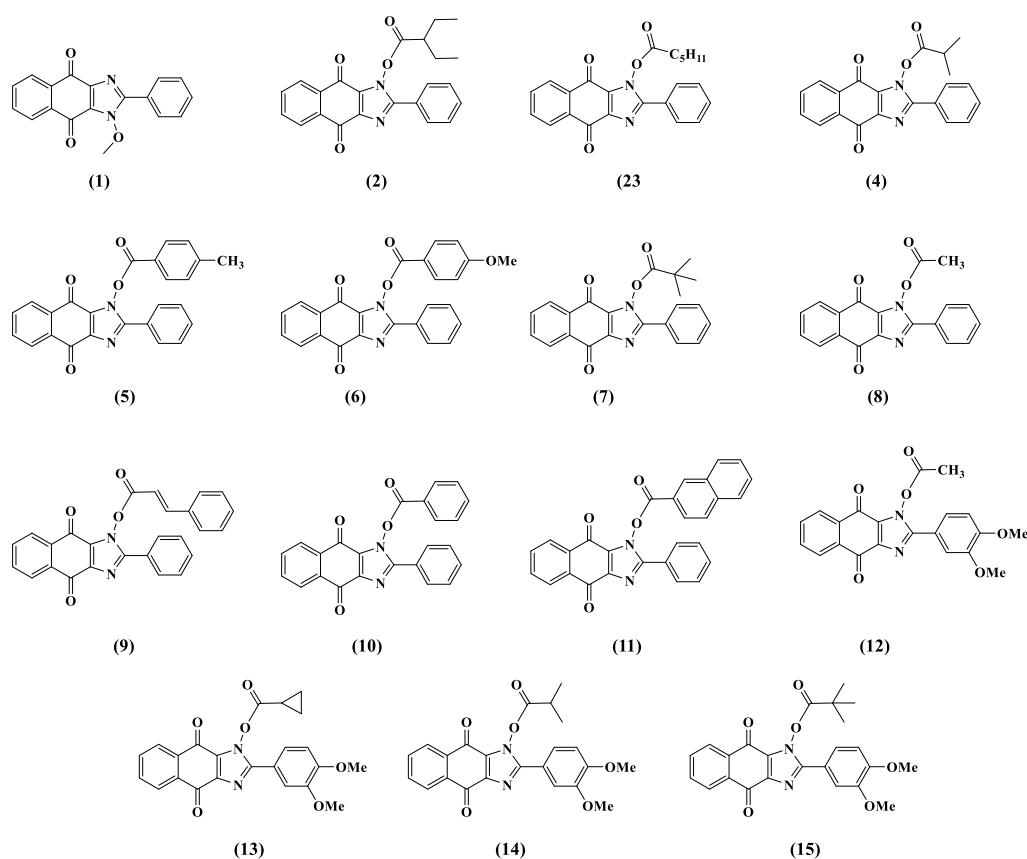
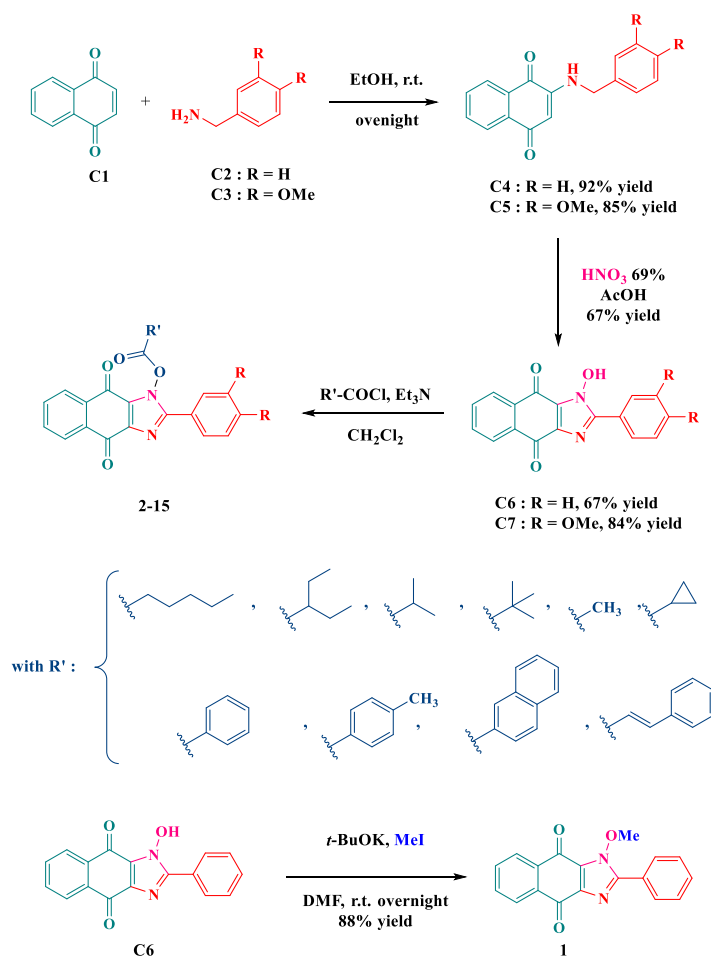


Figure 2. Structure of oxime-esters like structures 1-15.

In the present case, oxime-esters like structures 1-15 were obtained, differing from the oxime esters by the presence of an imidazolyl group connected to the photocleavable group. The two precursors of these structures (C6 and C7) could be prepared in two steps, first by Michael addition of the appropriate benzylamine derivatives (C2 and C3) on 1,4-naphthoquinone C1.[172–179] C4 and C5 could be obtained in 92 and 85% yield respectively. By a cyclization reaction done in the conditions previously reported by Lavrikova and coworkers using nitric acid and acetic acid,[136] the cyclized compounds C6 and C7 were obtained in 67 and 84% yield respectively. Finally, by esterification with the appropriate acid chlorides, compounds 2-15 could be obtained with reaction yields ranging between 71% for

compound 4 up to 95% for compound 11. Using these different acid chlorides, and based on the photomechanism of oxime esters, namely, the decarboxylation reaction, the generation of primary, secondary, tertiary aliphatic radicals, but also of stabilized and destabilized aryl radicals can thus be formed, evidencing the interest of this series of 15 oxime esters. As a reference compound, compound 1 was obtained by alkylation of the alcohol group using iodomethane and potassium *tert*-butoxide as the base (See Scheme 2).[177,180,181] Since its establishment, the concept of green chemistry has developed plethora of metrics for measuring the greenness of reactions and thus of the obtained products.[182] In this field, the E-factor that determines the ratio between the total waste (kg) / total product (kg) constitutes one of the metrics of green chemistry. For all these photoinitiators, a E-factor higher than 200 could be determined,[183,184] consistent with the environmental impact of fine chemistry and pharmaceutical chemistry.[184] Even if high E-factors can be determined, these values are acceptable, with regards to the value of products (i.e. photoinitiators that can be used at low content) and the scope of applications of photoinitiators/photopolymerization (3D-printing, dentistry with the dental restorations, medicines with the reconstruction of the structural and functional complexity of human tissues including protheses). To end, photopolymerization is nowadays used in aerospace and aeronautics, rendering such E-factors acceptable.



Scheme 2. Synthetic route to compounds 1-15.

Table 1. Reaction yields determined during the synthesis of compounds 2-15.

Compound	2	3	4	5	6	7	8
Yield	78	82	71	84	85	88	76
Compound	9	10	11	12	13	14	15
Yield	76	81	95	78	88	84	80

From the absorption viewpoint, introduction of methoxy groups on the phenyl ring induced a significant blueshift of the absorption spectra compared to the phenyl analogues (See Figure 3 and Table 2), since a shift by ca 55 nm could be detected for compounds 12-15 compared to compounds 2-11.

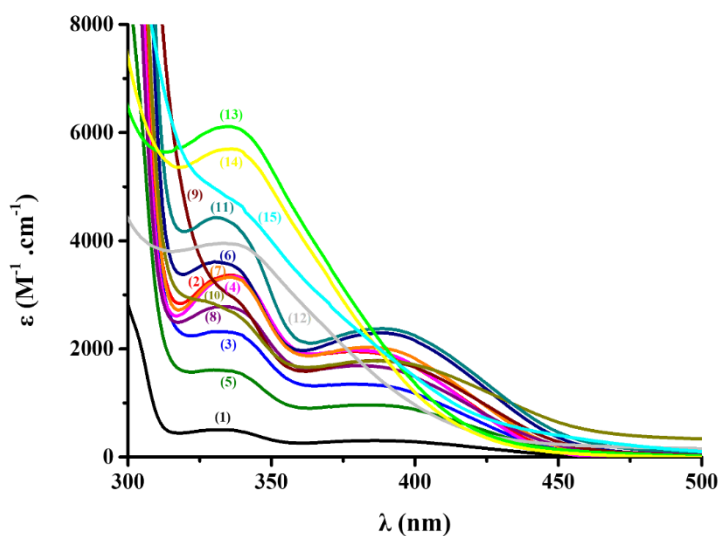


Figure 3. Absorption spectra of compounds 1-15 in acetonitrile. Reproduced with permission of Ref.[154]

Table 2. Absorption characteristics of compounds 1-15 in acetonitrile at different wavelengths.

PIs	λ_{\max} (nm)	ϵ_{\max} ($M^{-1}\cdot cm^{-1}$)	ϵ_{405} ($M^{-1}\cdot cm^{-1}$)	ϵ_{455} ($M^{-1}\cdot cm^{-1}$)
(1)	330	500	260	30
(2)	380	1950	1500	90
(3)	382	1350	1070	100
(4)	378	1980	1510	40
(5)	383	970	810	100
(6)	388	2300	2010	260
(7)	383	2000	1670	130
(8)	382	1700	1360	170
(9)	387	1800	1550	210
(10)	385	1800	1630	570
(11)	388	2370	2110	360

(12)	333	3960	810	220
(13)	334	6110	1100	120
(14)	336	5700	960	70
(15)	339	4670	1290	360

Despite this blueshift, all structures were appropriate candidates for photopolymerization experiments done at 405 and 455 nm.

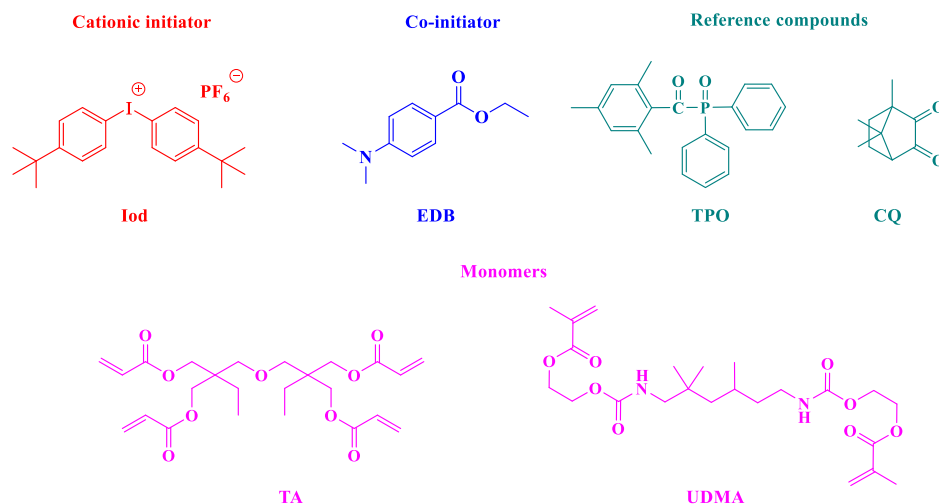


Figure 4. Structures of monomers and additives used with 1-15 as Type I photoinitiators.

Photopolymerization experiments done at 405 nm using (trimethylolpropane)tetraacrylate (TA) as the tetrafunctional monomer revealed the different photoinitiators to furnish lower monomer conversions in thin samples than TPO (0.5 wt%). A different behavior was found upon irradiation at 455 nm since compounds 2, 3, 4, 7 and 8 could outperform TPO. Thus, conversions of 80, 71, 83, 76 and 87% could be determined after 100s of irradiation contrarily to 61% for TPO. A similar trend could be determined in thick films. Here again, a few photoinitiators (compounds 2-4, 7, 8, 12 and 13) could furnish higher monomer conversions than diphenyl(2,4,6-trimethylbenzoyl)phosphine oxide (TPO) (See Table 3). While comparing compounds 8 and 12 bearing the same photocleavable groups, a strong influence of the substitution pattern was evidenced since compound 8 outperformed compound 12, irrespective of the polymerization conditions and the irradiation wavelengths. The lower reactivity of compound 12 compared to compound 1 can be assigned to the blueshifted absorption of compound 12, resulting in lower molar extinction coefficients at 405 and 455 nm (810 and $220 \text{ M}^{-1}\cdot\text{cm}^{-1}$ for compound 12 vs. 1360 and $170 \text{ M}^{-1}\cdot\text{cm}^{-1}$ for compound 8 at 405 and 455 nm respectively).

Table 3. Final conversions determined during the FRP of TA using 1-15 as monocomponent systems (0.5 wt%) after 100 s of irradiation with LEDs ($\lambda = 405$ and 455 nm).

PIs	Thin Samples	Thin Samples	Thick Samples	Thick Samples
	in laminate 405 nm	in laminate 455 nm	under air 405 nm	under air 455 nm
TPO	90%	61%	95%	77%
(1)	65%	48%	25%	1%
(2)	82%	80%	78%	78%
(3)	68%	71%	84%	81%
(4)	81%	83%	83%	85%
(5)	49%	55%	78%	74%
(6)	34%	53%	48%	68%
(7)	79%	76%	86%	80%
(8)	88%	87%	88%	84%
(9)	42%	24%	48%	65%
(10)	18%	32%	54%	54%
(11)	39%	32%	63%	66%
(12)	56%	65%	76%	78%
(13)	71%	73%	74%	78%
(14)	68%	59%	78%	61%
(15)	54%	48%	76%	67%

Among all structures investigated in this work, compound 8 proved to be the most efficient Type I photoinitiator. Notably, in thin films and upon excitation at 455 nm, compound 8 furnished a TA double bond conversion of 87%, higher than the conversions obtained with TPO (61%), the camphorquinone (CQ)/ ethyl dimethylaminobenzoate (EDB) system (63%) or titanocene (76%) at similar concentrations (See Figure 5). Besides, if excellent TA conversions could be obtained by using 0.5 wt% photoinitiators, this photoinitiator content is comparable than that used with oxime esters bearing other chromophores such as coumarins (0.1 wt%),^[185] 5,12-dialkyl-5,12-dihydroindolo[3,2-*a*]carbazoles,^[186] pyrene or anthracene.^[187] These structures thus do not exhibit an improved reactivity compared to those previously reported in the literature.^[188] But considering that the use of such naphthoquinone derivatives was unprecedented in the literature in photopolymerization, from my viewpoint, examination of their photoinitiating abilities was primordial, with aim at identifying highly efficient photoinitiators activable at 405 nm or at longer wavelength.

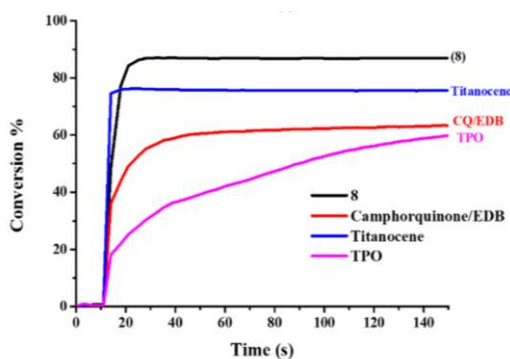
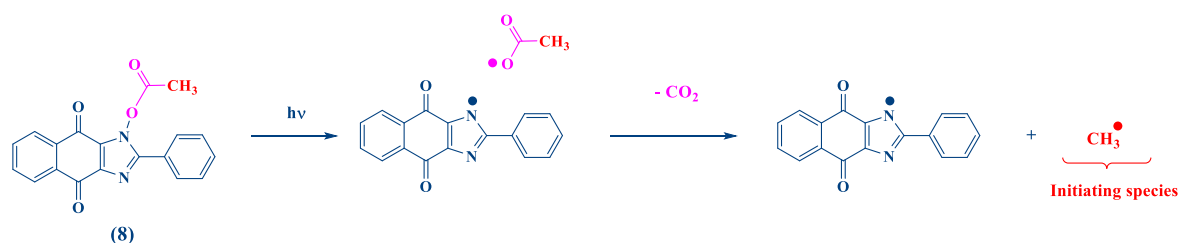


Figure 5. TA double bond conversions obtained with different photoinitiating systems upon excitation at 455 nm in thin films: compound 8 (0.5% w/w), CQ/EDB (0.5%/0.5% w/w); TPO (0.5% w/w) and titanocene (0.5% w/w). Reproduced with permission of Ref.[154]

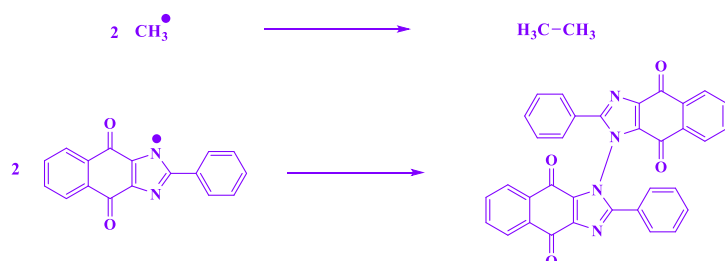
By theoretical calculations, the bond dissociation energy (BDE) as well as the energy of the triplet state could be determined. Parallel to this, energy level of the singlet excited state was estimated from the crossing point of the UV-visible absorption and photoluminescence spectra. As shown in Table 4, a more negative value for the enthalpy of cleavage was determined for the photocleavage of the N-O bond from the singlet state compared to the triplet state, evidencing that the cleavage was certainly occurring from the singlet excited state. By infrared spectroscopy, release of CO₂ was evidenced by the appearance of a peak at 2337 cm⁻¹, and these results were confirmed by electron spin resonance spin trapping (ESR-ST) experiments. By combination of these complementary techniques, the mechanism depicted in the Scheme 3 was proposed. Subsequent to the photocleavage of the N-O bond upon photoexcitation, an homolytic cleavage of the N-O can occur, producing alkyloxy radicals and imidazolyl radicals. Subsequent to fragmentation, a decarboxylation can occur, generating alkyl radicals. Interestingly, among all alkyl radicals, the methyl radicals are undoubtedly the most reactive ones, and this point has been evidenced by different research groups with various oxime esters.[149,156–158,160–162,189,190] Parallel to the logical reaction pathway proposed by Lalevée and coworkers, speculations can also be proposed concerning the occurrence of self-recombination reactions (See Supporting information). Notably the recombination of alkyl radicals subsequent to decarboxylation can be suggested. Similarly, imidazolyl radicals can also dimerize, even if no proof of occurrences of such reactions has been given by the authors (See Scheme 3). Even if the determination of occurrence of self-recombination reactions is of interest for photopolymerists interested in controlled photopolymerization, such investigations become out of interest for photocrosslinking, all side-reactions being beneficial for the crosslinkage of polymer chains.

Table 4. Bond dissociation energy BDE (N–O), triplet state energy E_{T1} , enthalpy ($\Delta H_{\text{cleavage}T1}$) of cleavage from T_1 ($\Delta H_{\text{cleavage}T1} = \text{BDE} - E_{T1}$), enthalpy ($\Delta H_{\text{cleavage}S1}$) of cleavage from S_1 ($\Delta H_{\text{cleavage}S1} = \text{BDE} - E_{S1}$), and excited state lifetime.

PIs	BDE (kcal/mol)	E_{S1} (kcal/mol)	$\tau_0(S_1)$ (ns)	$\Delta H_{\text{cleavage}S1}$ (kcal/mol)	E_T (kcal/mol)	$\Delta H_{\text{cleavage}T1}$ (kcal/mol)
(1)	41.78	62.3	3.45	-20.51	50.98	-9.2
(2)	35.76	63.5	2.49	-27.74	50.57	-14.81
(3)	36.54	63.8	2.46	-27.26	50.69	-14.15
(4)	34.95	63.5	1.76	-28.55	50.76	-15.81
(5)	34.90	62.2	2.75	-27.3	50.77	-15.87
(6)	34.94	62.6	2.63	-27.66	50.76	-15.82
(7)	35.03	62.8	3.09	-27.77	50.53	-15.50
(8)	36.19	65.13	2.36	-28.94	50.71	-14.52
(9)	34.92	64.3	2.41	-29.38	50.47	-15.55
(10)	34.87	61.8	2.56	-26.93	50.75	-15.88
(11)	34.78	62.6	2.57	-27.82	50.77	-15.99
(12)	32.68	-	-	-	47.12	-14.44
(13)	32.38	-	-	-	47.56	-15.18
(14)	31.41	-	-	-	47.29	-15.88
(15)	31.89	-	-	-	47.82	-15.93



Speculations about self-recombination reactions



Scheme 3. Mechanism of photoinitiation with the naphthoquinone-imidazolyl esters and unverified speculations about self-recombination reactions.

Interest of the most reactive structure i.e. compound 8 was demonstrated during the direct laser write experiments done at 405 nm. As shown in Figure 6, 3D patterns with an excellent spatial resolution could be obtained using TA as the monomer.

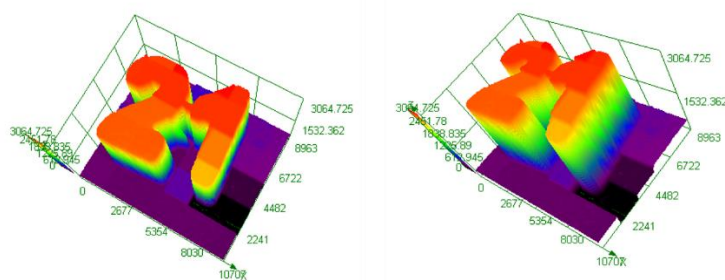


Figure 6. 3D pattern obtained using compound 8 as the Type I photoinitiator. Reproduced with permission of Ref.[154]

In 2024, a different strategy was used to prepare a series of Type I photoinitiators starting from 2-phenyl-1*H*-naphtho[2,3-*d*]imidazole-4,9-dione scaffold.[191] Contrarily to compounds 2-15 in which the photocleavable group was introduced close to the naphthoquinone chromophore, in the present case, the oxime ester groups were introduced on the opposite side of the naphthoquinone imidazolyl group so that the impact of the distance between the chromophore and the photocleavable group could be examined. A series of nine structures C1-C9 were prepared, differing by the group introduced on the oxime ester side (See Figure 7).

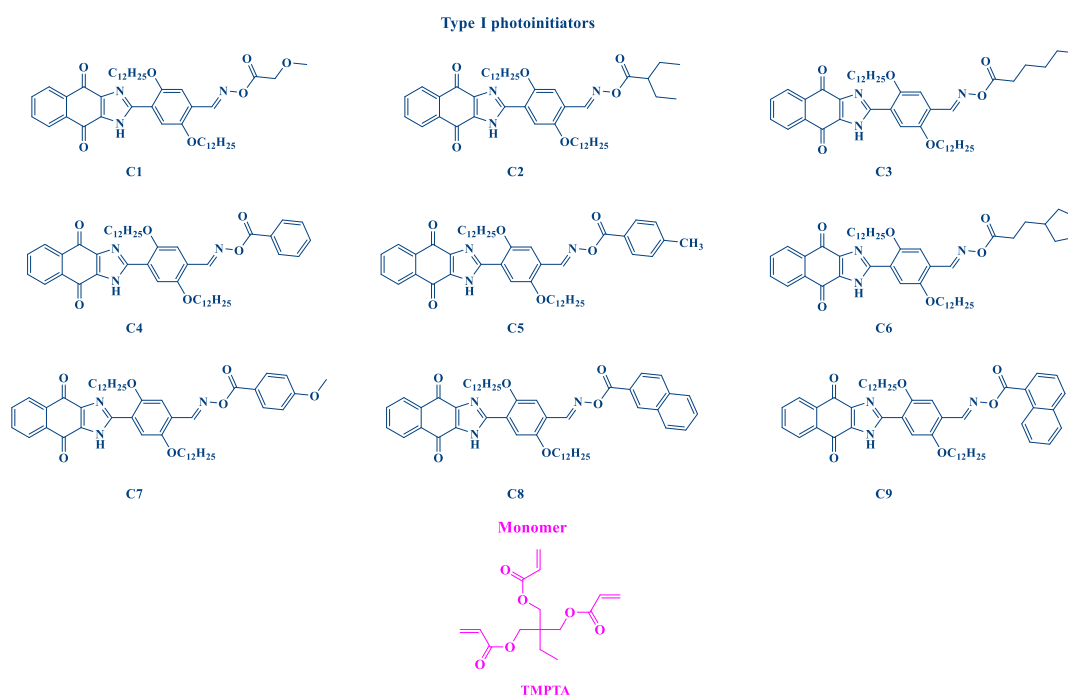
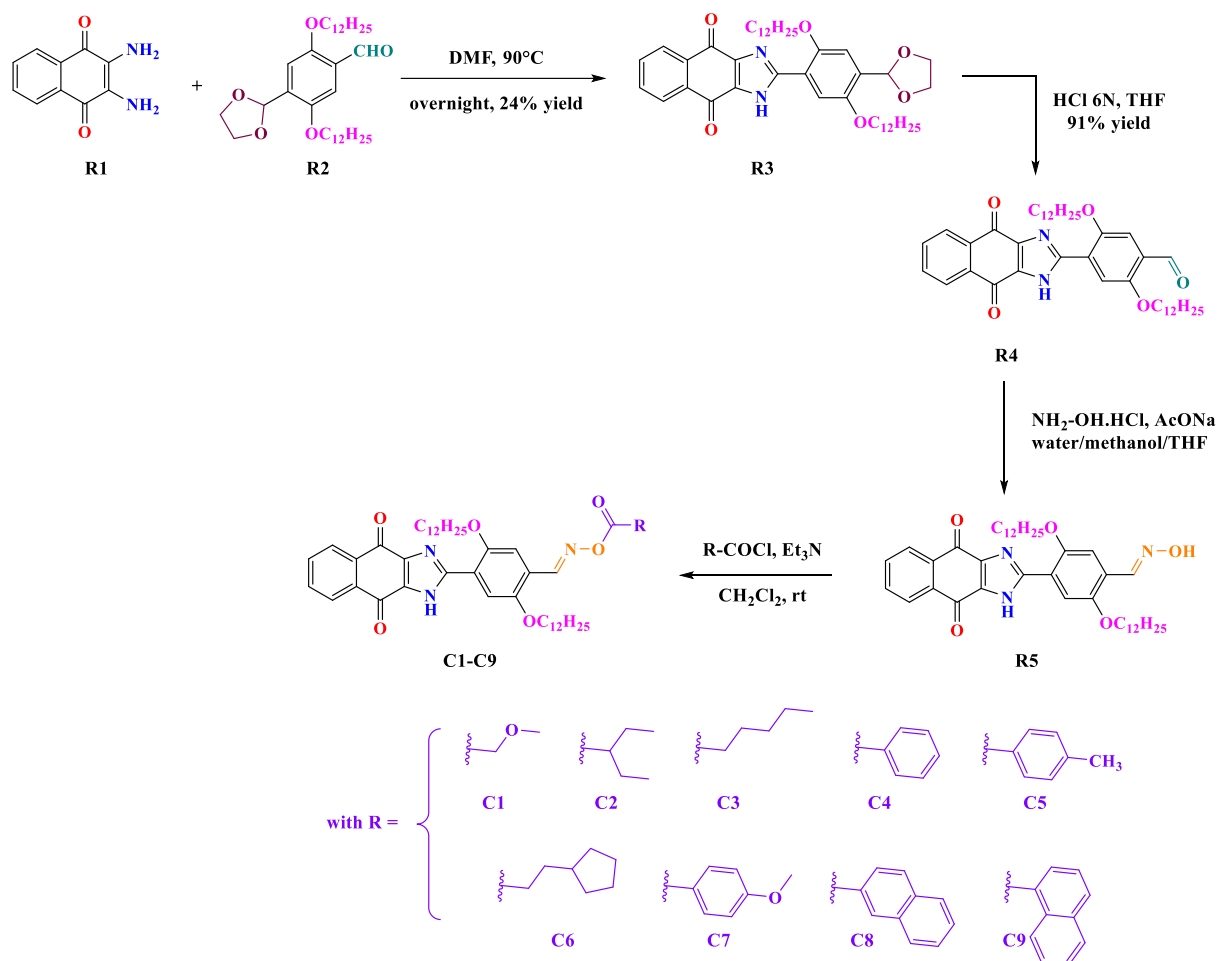


Figure 7. Series of oxime esters based on the 2-phenyl-1*H*-naphtho[2,3-*d*]imidazole-4,9-dione scaffold and the monomer used in this study (TMPTA).

The nine oxime esters could be prepared in four steps, starting from 2,3-diaminonaphthalene-1,4-dione R1[192–201] and 4-(1,3-dioxolan-2-yl)-2,5-bis(dodecyloxy) benzaldehyde R2. The condensation product R3 could be isolated in 24% yield. After hydrolysis of the acetal in acidic conditions, R4 was converted as an oxime by reaction with hydroxylamine hydrochloride in basic conditions. Finally, R5 could be esterified with different acid chloride, providing C1-C9 (See Scheme 4). For the different aforementioned photoinitiators C1-C9, a E-factor higher than 200 could be calculated.[183,184] The amount of waste byproducts thus formed during the synthesis of the photoinitiators is consistent with that produced in fine chemical and specialty chemical industry.



Scheme 4. Synthetic route to C1-C9.

As anticipated, the group introduced on the oxime ester side did not influence the position of the absorption spectra and similar absorption maxima were determined for C1-C9, peaking between 372 and 376 nm in dichloromethane (See Figure 8 and Table 5). Only weak variations of the molar extinction coefficients could be determined between oxime esters. Based on their absorption characteristics, the different compounds were tested as photoinitiators upon excitation at 365, 385 and 405 nm for the FRP of trimethylolpropane triacrylate (TMPTA).

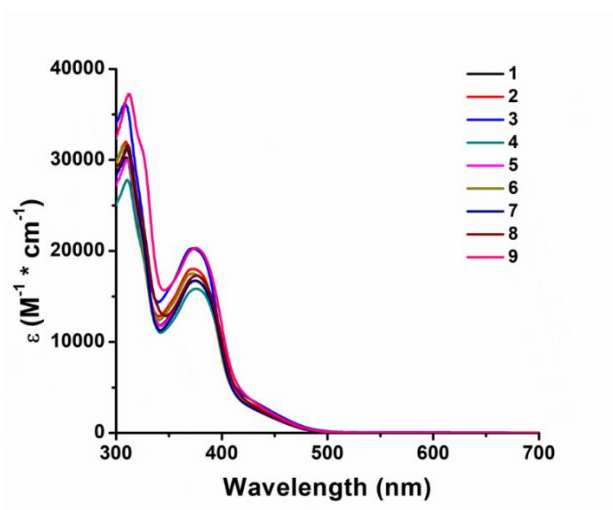


Figure 8. Absorption spectra of C1-C9 in dichloromethane. Reproduced with permission of Ref.[191]

Table 5. Absorption characteristics of C1-C9 in dichloromethane.

PIs	λ_{\max} (nm)	ϵ_{\max} ($M^{-1}\cdot cm^{-1}$)	$\epsilon_{@405\text{ nm}}$ ($M^{-1}\cdot cm^{-1}$)
C1	375	16710	6530
C2	373	18020	6390
C3	372	20280	7190
C4	375	15850	6680
C5	374	16700	6930
C6	372	17510	6200
C7	376	16730	6580
C8	376	17270	7640
C9	375	20320	8800

Noticeably, the final monomer conversions obtained with oxime esters bearing alkyl groups on the oxime ester side furnished higher monomer conversions than their aromatic analogues. If all oxime esters exhibited excellent light absorption properties at 365 nm, their photoinitiating abilities were low. Conversely, at 385 and 405 nm, the monomer conversions increased for almost all Type I photoinitiators despite a severe reduction of the molar extinction coefficients, evidencing that the reactivity of oxime esters was disconnected from the molar extinction coefficients (See Table 6). Besides, even at 405 nm, the TMPTA double bond conversions remained low, ranging between 20% for C1 and 63% for C4 in thin samples. The only remarkable structures of this series were C8 and C3, enabling to reach a TMPTA double bond conversion of 72 and 865% respectively in thin samples. In thick samples, a reduction of the monomer conversion was detected, resulting from inner filter effects impeding light penetration within the resins. The lack of reactivity is directly related to the distance between the chromophore and the photocleavable group. Due to the distance between the naphthoquinone moiety and the oxime ester group, efficiency of the energy

transfer between the two partner is considerably reduced, adversely affecting the polymerization efficiency.

Table 6. TMPTA double bond conversions determined by using C1-C9 (0.1 wt%) after 300 s of irradiation with different LEDs (365, 385 and 405 nm).

PIs	Thin samples	Thick samples	Thick samples	Thick samples
	in laminate	under air	under air	under air
	405 nm	405 nm	365 nm	385 nm
C1	20%	49%	15%	43%
C2	34%	49%	7%	28%
C3	85%	53%	3%	24%
C4	63%	44%	1%	5%
C5	62%	39%	1%	16%
C6	26%	45%	4%	32%
C7	39%	38%	1%	9%
C8	72%	29%	2%	14%
C9	62%	30%	1%	10%

Considering that the best monomer conversions were obtained at 405 nm but were still low for a monomer such as TMPTA, the different oxime esters were tested in combination with EDB and Iod at this specific wavelength, and thus tested as Type II photoinitiators. As shown in Table 7, a significant improvement of the monomer conversions could be detected while using the dye/Iod and dye/EDB combinations. The best performances were obtained with the two-component dye/EDB systems. Thus, in thick films and under air, an increase of the TMPTA double bond conversion from 48% as monocomponent system up to 68 and 74% were determined for the two-component C1/Iod and C1/EDB photoinitiating systems respectively. The highest improvement of the monomer conversions was determined for C9, increasing from 62% (as monocomponent system) to 93% with the two-component dye/Iod system in thin films (See Figure 9).

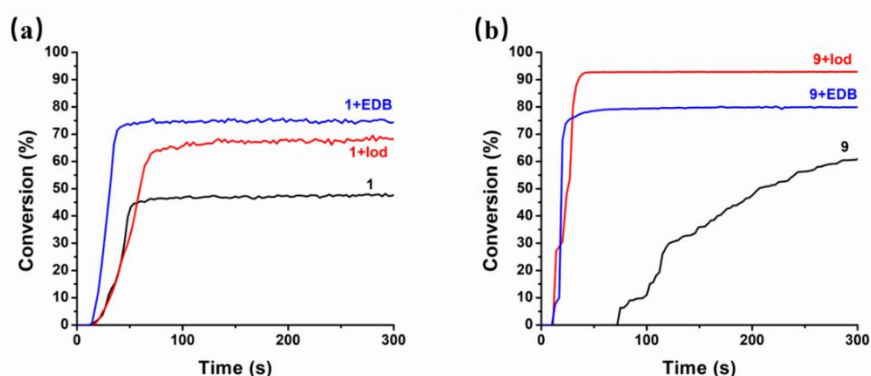
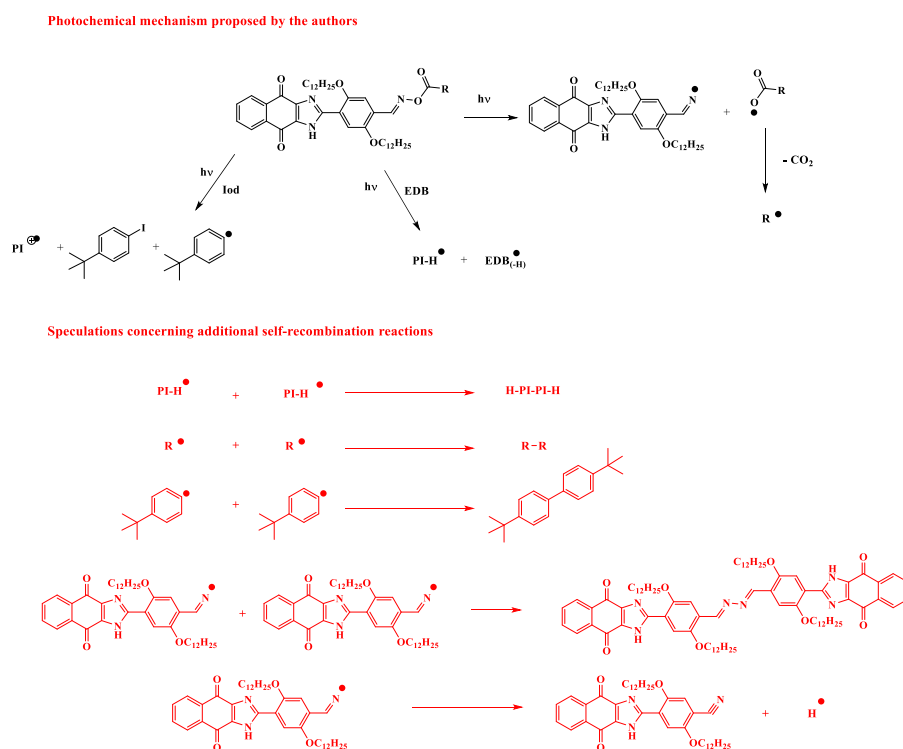


Figure 9. Photopolymerization profiles of TMPTA upon irradiation at 405 nm using a) C1 (0.1 wt%), C1/Iod (0.1%/2% w/w) and C1/EDB (0.1%/2% w/w) in thick films and under air; b) C9 (0.1 wt%), C9/Iod (0.1%/2% w/w) and C9/EDB (0.1%/2% w/w) in thin films and in laminate. Reproduced with permission of Ref.[191]

Table 7. TMPTA double bond conversions obtained by using dye/Iod (0.1%/2%, w/w) and dye/EDB (0.1%/2% w/w) after 300 s of irradiation with a LED@405 nm.

PIs	Thin samples (25 μm) in laminate		Thick samples (1.5 mm) under air	
	Compounds/Iod	Compounds/EDB	Compounds/Iod	Compounds/EDB
C1	38%	48%	68%	74%
C2	67%	40%	61%	72%
C3	82%	71%	57%	72%
C4	54%	85%	43%	57%
C5	85%	52%	57%	63%
C6	48%	87%	65%	72%
C7	78%	50%	48%	68%
C8	88%	62%	56%	69%
C9	93%	80%	46%	62%

By combining the results obtained during the steady state photolysis and electron spin resonance spin trapping experiments, the photochemical mechanism could be elucidated. Thus, when used as monocomponent systems, a classical photocleavage of oxime esters could be evidenced, with the cleavage of the N-O bond generating an alkyloxy radical and an iminyl radical. When used in combination with Iod and EDB, Ph• radicals[202–206] and EDB_(-H)• radicals[207–210] are respectively formed, enabling to initiate the FRP of TMPTA (See Scheme 5).



Scheme 5. Photochemical mechanisms occurring with C1-C9 as the oxime esters and speculations concerning the occurrence of additional self-recombination reactions not detailed by the authors.

But speculations concerning additional self-recombination reactions can also be proposed. For instance, PI-H• can self-dimerize, impeding the propagation of the polymerization process. Similarly, after photocleavage and decarboxylation reactions of oxime esters, R• can recombine, producing R-R structures. Concerning iminyl radicals, these structures can also contribute to polymerization,[161] even if recent studies have demonstrated these structures to be capable to dimerize or to generate nitrile derivatives (See Scheme 5).[211] Besides, no HPLC analyses supports such occurrences. To end, radicals formed by the photoinduced reduction of the iodonium salts can also dimerize (when oxime esters are used as Type II photoinitiators), as shown in Scheme 5. However, once again, identification of such structures has not been carried out by the authors and these conjectures are pure speculations. Besides, my opinion concerning the occurrence of additional self-recombination reactions is that in the coming years, no works should be published without investigating this point. The formation of side-products during photopolymerization is more important to investigate than the polymer itself.

2.2. Type II photoinitiators

As evidenced with oxime esters C1-C9, naphthoquinone-imidazolyl derivatives can act as efficient photosensitizers for an iodonium salt, improving in turn the monomer conversions. In the case of Type I photoinitiators of low photoinitiating ability, these structures besides contain a chromophore that can be used as a photosensitizer for additives such as Iod or EDB. These low-reactive Type I photoinitiators are thus recycled as Type II photoinitiators. In light of these results, a more straightforward approach consists in directly designing Type II photoinitiators using the 2-phenyl-1*H*-naphtho[2,3-*d*]imidazole-4,9-dione scaffold. In 2023, a series of naphthoquinone derivatives (Dye 1-Dye 10) specifically designed for acting as Type II photoinitiators was proposed by Lalevée and coworkers (See Figure 10).[191]

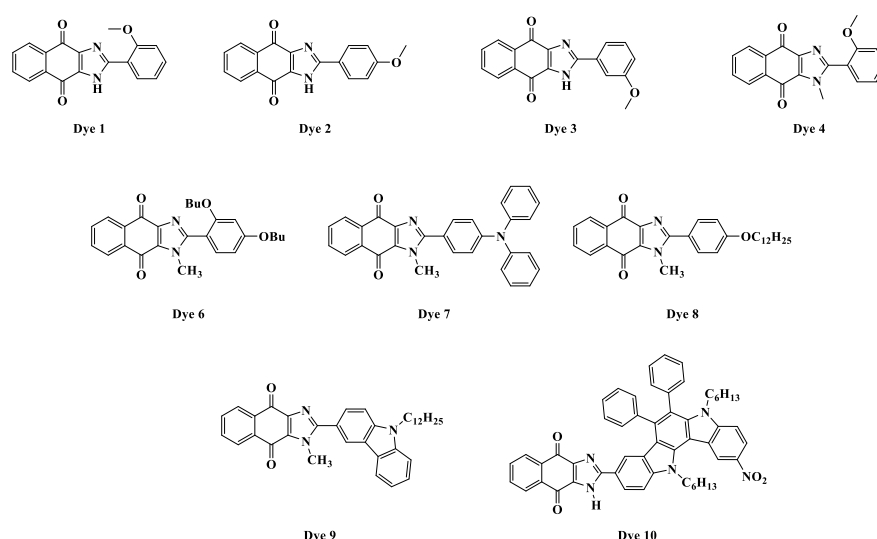
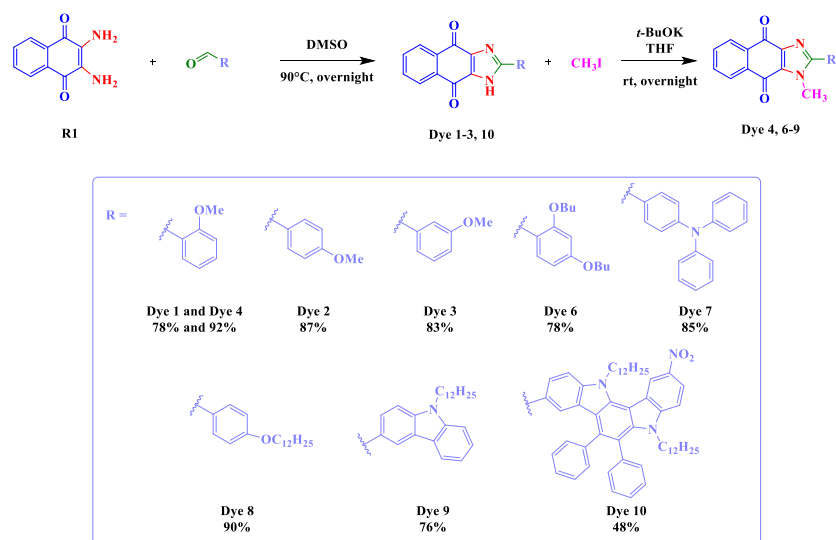


Figure 10. Structures of naphthoquinone-imidazolyl derivatives investigated as Type II photoinitiators.

The synthesis of Dye 1-Dye 4, Dye 6-Dye 10 was straightforward, and the different dyes could be obtained after a one-step imidazole ring formation of 2,3-diaminonaphthalene-1,4-

dione R1 with the appropriate aldehyde, furnishing the dyes with reaction yields ranging between 48% for Dye 10 up to 87% for Dye 2.[133–135] In the second step, and in order to improve the solubility of the dyes, the desired compounds Dye 4, Dye 6–Dye 9 were obtained via the alkylation of the imidazole ring with iodomethane in the presence of a base (See Scheme 6).[135,212,213] For all these photoinitiators, a E-factor higher than 200 could be determined, comparable to that determined for the other aforementioned naphthoquinone structures.[183,184]



Scheme 6. Synthesis of Dye 1-Dye 4, Dye 6-Dye 10.

All dyes exhibited a broad absorption extending up 600 nm (See Figure 11). Besides, these structures were only tested at 405 nm for polymerization experiments. The highest molar extinction coefficient was determined for Dye 10, bearing a 5,12-dihexyl-6,7-diphenyl-5,12-dihydroindolo[3,2-*a*]carbazole moiety (See Figure 11 and Table 8). This is directly related to the polyaromaticity of the group attached to this structure. Thus, at 405 nm, a molar extinction coefficient as high as 19 000 M⁻¹.cm⁻¹ could be determined for Dye 10.

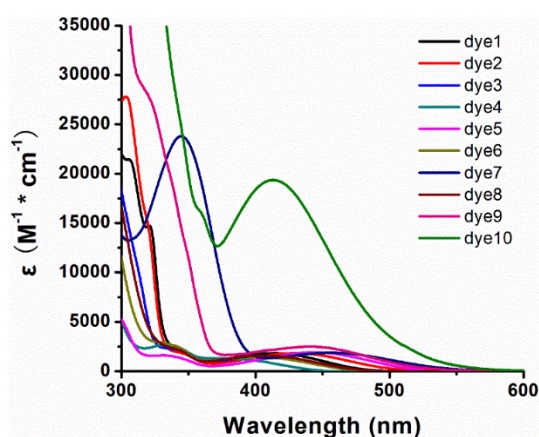
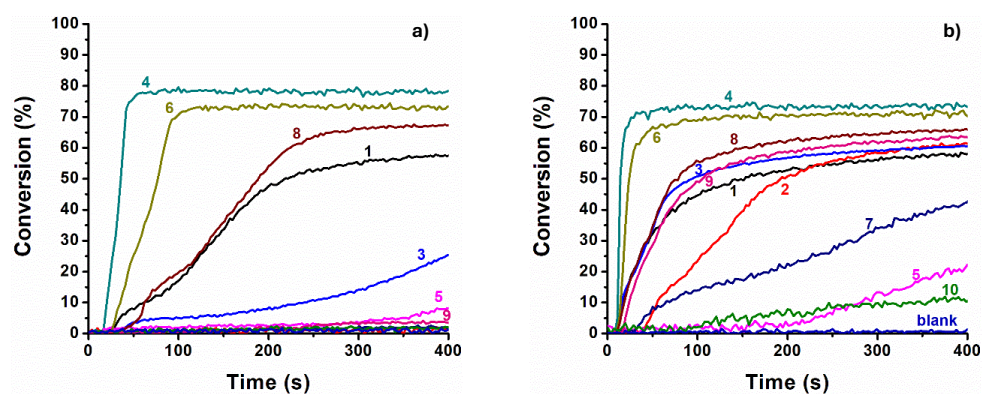


Figure 11. Absorption spectra of Dye 1-Dye 4, Dye 6-Dye 10 in chloroform. Reproduced with permission of Ref.[191]

Table 8. Absorption characteristics of Dye 1-Dye 4, Dye 6-Dye 10 in chloroform.

Compounds	$\lambda_{\max}(\text{nm})$	$\epsilon_{\max}(\text{M}^{-1}\cdot\text{cm}^{-1})$	$\epsilon_{@405\text{nm}}(\text{M}^{-1}\cdot\text{cm}^{-1})$
Dye 1	414	1840	1790
Dye 2	430	1850	1540
Dye 3	410	1470	1460
Dye 4	380	1300	1000
Dye 6	401	1460	1450
Dye 7	456	1890	1380
Dye 8	405	1600	1600
Dye 9	441	2510	2060
Dye 10	413	19370	19000

Photolysis experiments done at 405 nm with the two-component dye/Iod, dye/EDB systems and the three-component dye/Iod/EDB revealed the photolysis rate to be slow for the dye/Iod combination. Notably, no photolysis could be detected for the dye alone or the dye/Iod combination after 300 s of irradiation at 405 nm. In contrast, a slow photolysis rate was obtained with the dye/EDB combination (around 300 s with Dye 1), evidencing that the dyes were easier to reduce than oxidize. Finally, the photolysis rate was greatly improved with the three-component system and a complete photolysis of the solution could be detected within 20 s (notably with Dye 1 for which the fastest photolysis rate was determined). A different behavior was found for Dye 4. In this case, the photolysis rate for the Dye 4/Iod combination was faster than that determined for the Dye 4/EDB system and even outperformed the photolysis rate of the three-component Dye 4/Iod/EDB system. Considering that Dye 1 and Dye 4 only differ by the alkylation of the imidazole group, it was thus concluded that a minor structural variation on the naphthoquinone-imidazole group could drastically modify the reactivity of the dyes while letting the absorption characteristics almost unchanged. When tested as photoinitiators of polymerization for the FRP of TMPTA, the trend of reactivity determined in solution during the photolysis experiments were different from those obtained during the polymerization of TMPTA. Thus, if the polymerization rate was higher for the Dye/EDB combination, in turn, higher monomer conversions were obtained with the dye/Iod systems (See Figure 12).

**Figure 12.** Polymerization profiles of TMPTA in thick films under air upon excitation at 405nm using (a) dyes/Iod (0.2%/2% w/w) b) dyes/EDB (0.2%/2% w/w). Reproduced with permission of Ref.[191]

Among all structures investigated, Dye 4, Dye 6 and Dye 8 furnished the highest TMPTA double bond conversions (higher than 65% after 400 s of irradiation). By using the three-component Dye/Iod/EDB systems, an improvement of the monomer conversion was detected, consistent with the photolysis experiments. In order to determine the role of dyes in photoinitiation, blank experiments were done with the two-component Iod/EDB system, at the same concentrations than that used in the three-component systems. In this case, a TMPTA double bond conversion of 85% was obtained with the blank experiment, higher than that obtained with the three-component systems (See Figure 13). However, the polymerization rate was much faster with the three-component systems, evidencing the role of the dyes in the generation of initiating species. If excellent TMPTA double bond conversions could be obtained with the three-component systems, as a drawback of this strategy, no photobleaching could be detected so that colored polymer films were obtained after polymerization (See Figure 13).

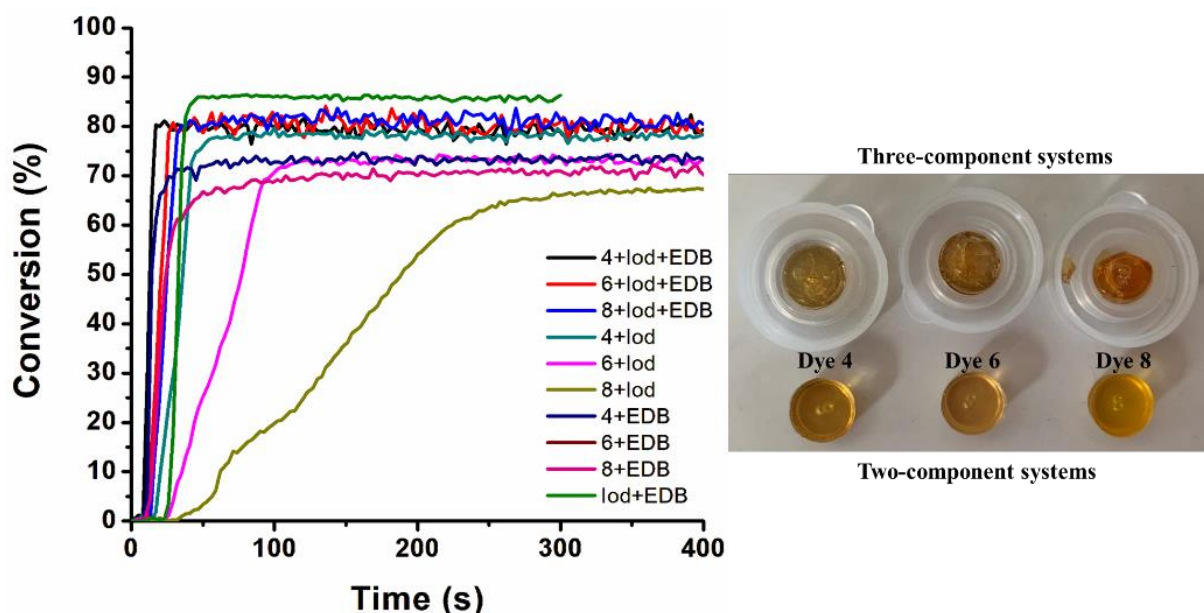


Figure 13. TMPTA double bond conversions obtained with different two and three-component systems upon excitation at 405 nm. Reproduced with permission of Ref.[191]

Comparisons with two other benchmark photoinitiators i.e. benzophenone (BP) and ITX revealed Dye 4 to furnish TMPTA double bond conversions on par with that obtained with BP and ITX using the two-component dye/Iod systems while using 0.1 or 0.2 wt% photoinitiator. However, by using a photoinitiator content as low as 0.05%, a TMPTA double bond conversion of ca. 80% could be still obtained with the Dye 4/Iod (0.05%/2% w/w) system (See Figure 14), whereas BP and ITX were ineffective at such concentration. The superiority of Dye 4 in photoinitiation was thus demonstrated.

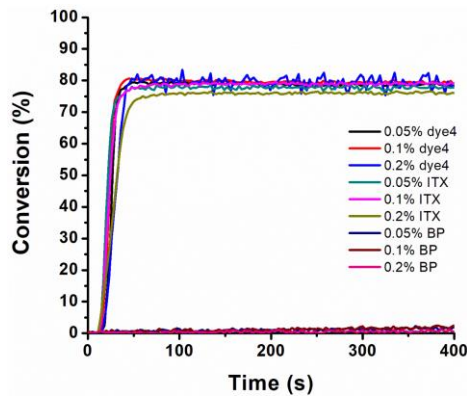


Figure 14. TMPTA double bond conversions obtained with different two-component dye/Iod photoinitiating systems upon excitation at 405 nm. Reproduced with permission of Ref.[191]

Interest of Dye 4 as a photosensitizer was finally demonstrated during direct laser write (DLW) experiments. Using different two-component dye/Iod and dye/EDB systems, the 3D patterns obtained with Dye 4 were better defined than those obtained with ITX (See Figure 15).

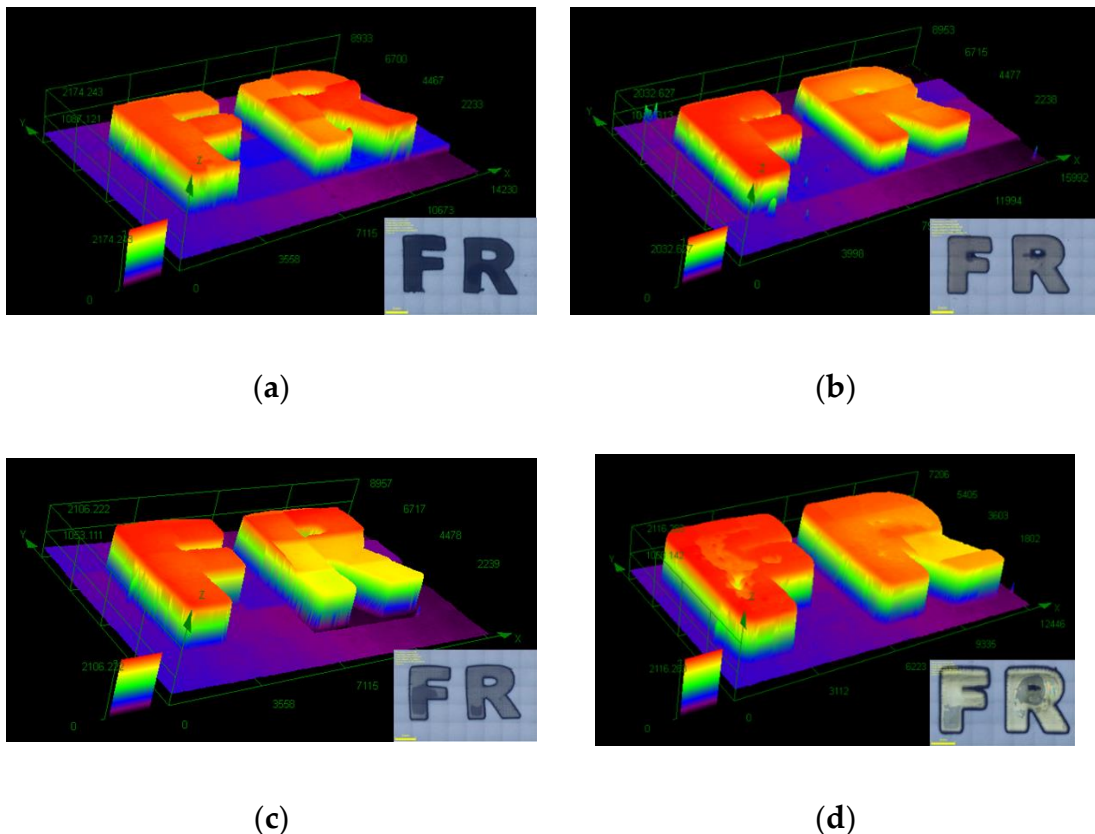


Figure 15. 3D patterns obtained with the two-component (a) dye 4/Iod; (b) dye 4/EDB; (c) ITX/Iod; (d) ITX/EDB systems and examined by optical microscopy. Reproduced with permission of Ref.[191]

3. Derivatives of 2-phenylnaphtho[2,3-*d*]thiazole-4,9-dione

3.1. Type I photoinitiators

If various derivatives of 2-phenyl-1*H*-naphtho[2,3-*d*]imidazole-4,9-dione have been designed as type I and type II photoinitiators, the related structures i.e. 2-phenylnaphtho[2,3-*d*]thiazole-4,9-diones have also been investigated for this purpose. Interest of 2-phenylnaphtho[2,3-*d*]thiazole-4,9-diones compared to 2-phenyl-1*H*-naphtho[2,3-*d*]imidazole-4,9-diones relies in the absence of the NH group, greatly improving the solubility of these derivatives. Additionally, by replacing the five-membered ring imidazole by a thiazole group, no acidic proton is present in the structure, what can drastically modify the reactivity of photoinitiators. In 2024, a series of eight 2-phenylnaphtho[2,3-*d*]thiazole-4,9-diones was designed and tested as Type I photoinitiators (See Figure 16).[214]

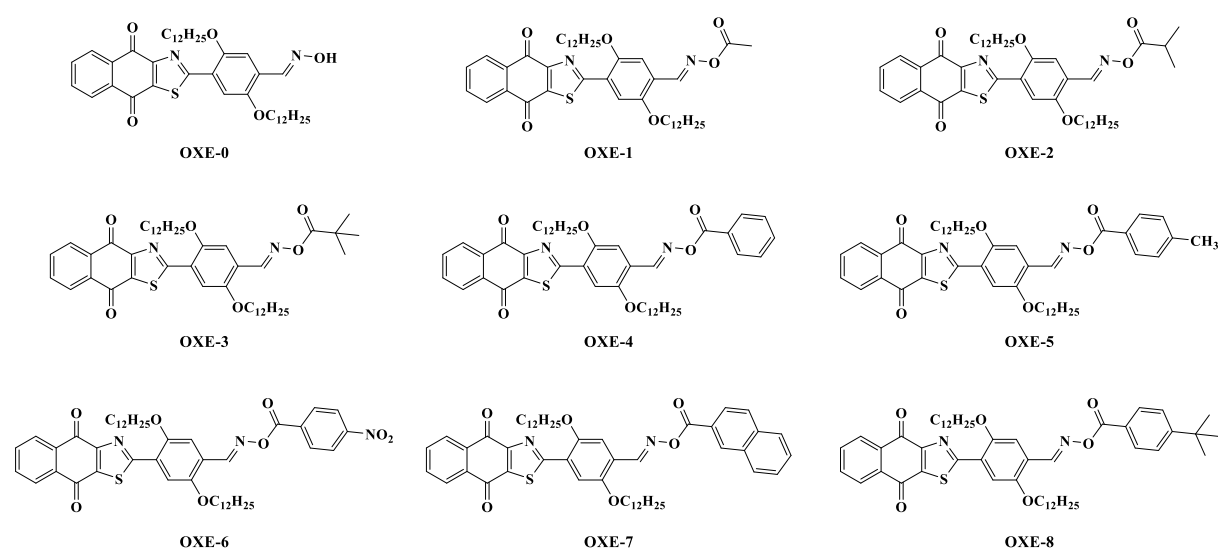
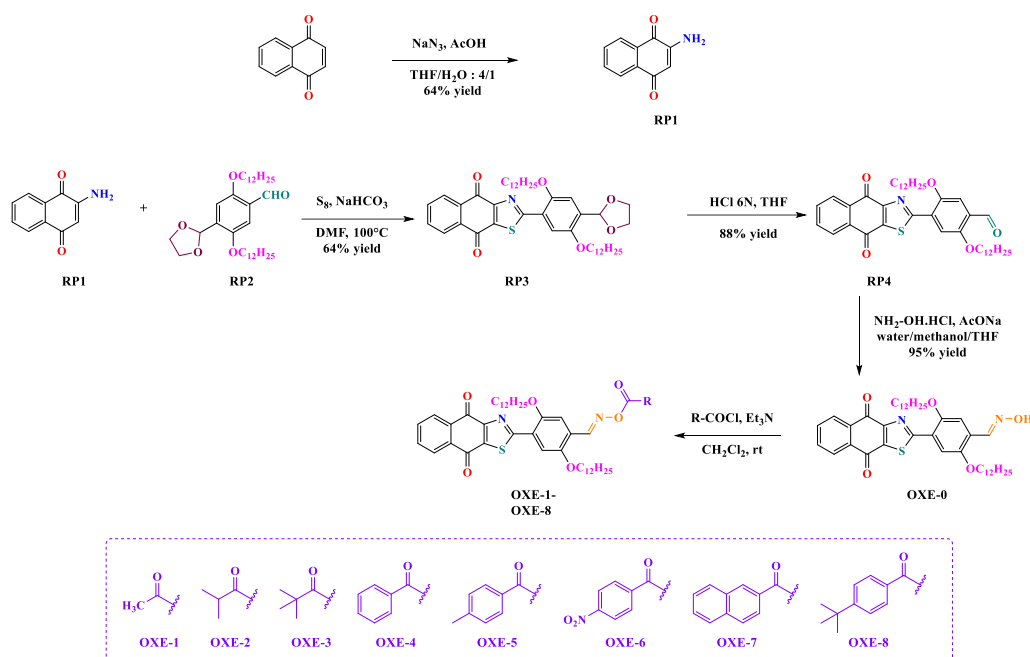


Figure 16. Structures of OXE-1 and OXE-8 designed as Type I photoinitiators.

Compared to the previous 2-phenyl-1*H*-naphtho[2,3-*d*]imidazole-4,9-dione derivatives C1-C9, a different synthetic route had to be used for the design of OXE-1-OXE-9. Starting from the biosourced 1,4-naphthoquinone, aminonaphthalene-1,4-dione RP1 could be prepared in one step starting from 1,4-naphthoquinone and sodium azide, furnishing the product in 64% yield.[215] By reaction of RP1 and 4-(1,3-dioxolan-2-yl)-2,5-*bis*(dodecyloxy)benzaldehyde RP2 in the presence of S8 and NaHCO₃, the intermediate RP3 could be prepared in 64% yield.[137] By treatment of RP3 under acidic conditions, RP4 could be obtained in 88% yield. Then, the oxime group was introduced using cheap and easily available reagents, using the procedure developed by Lachman and Noller in 1930 (See Scheme 7).[216] The oxime OXE-0 could be prepared in almost quantitative yields. Finally, by esterification of OXE-0 using the appropriate acid chlorides and a base, OXE-1-OXE-8 could be obtained with reaction yields ranging between 74% for OXE-6 and 92% for OXE-4. For all these photoinitiators, a E-factor higher than 200 could be determined, comparable to that determined for other naphthoquinone structures.[183,184]



Scheme 7. Synthesis of OXE-1-OXE-8.

While comparing the absorption properties of OXE-1-OXE-8 with that of C1-C9, a redshift of the absorption maximum by ca. 20 nm could be determined for the thiazole derivatives. Thus, absorption maxima located between 393 and 397 nm could be determined for the OXE-1-OXE-8 series contrarily to 372-376 nm for the C1-C9 series (See Tables 5 and 9, Figure 16).

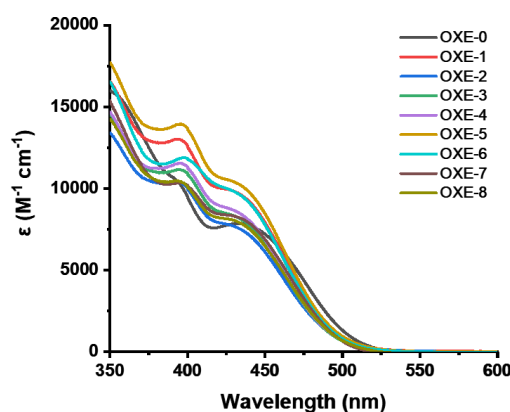


Figure 16. Absorption spectra of OXE-01~08 in DCM. Reproduced with permission of Ref. [214]

This redshift of the absorption maxima for the thiazole series compared to the imidazole series can be assigned to the specific electronic distribution detected for the frontier orbitals of the thiazole series. As shown in Figure 17, the highest occupied molecular orbitals (HOMO) of OXE-1-OXE-3 extend from the electron-donating *bis*-decyloxyphenyl group up to the thiazole group, increasing the energy level of the HOMO levels and thus decreasing the HOMO-LUMO gap (where LUMO stands for lowest unoccupied molecular orbital). Indeed,

the thiazole ring exhibit a higher electron-donating ability than the imidazole group, destabilizing the HOMO energy levels.

Table 9. Light absorption properties of OXEs in DCM.

PI	λ_{\max} (nm)	ϵ_{\max} ($M^{-1}.cm^{-1}$)	ϵ_{405} ($M^{-1}.cm^{-1}$)	ϵ_{450} ($M^{-1}.cm^{-1}$)
OXE-0	393	10000	8500	7200
OXE-1	393	13000	11700	7900
OXE-2	394	10300	9300	6100
OXE-3	395	11100	10200	6600
OXE-4	396	11500	10600	6800
OXE-5	394	14000	12800	8500
OXE-6	397	12000	11400	7700
OXE-7	396	10300	9700	6900
OXE-8	394	10500	9500	6500

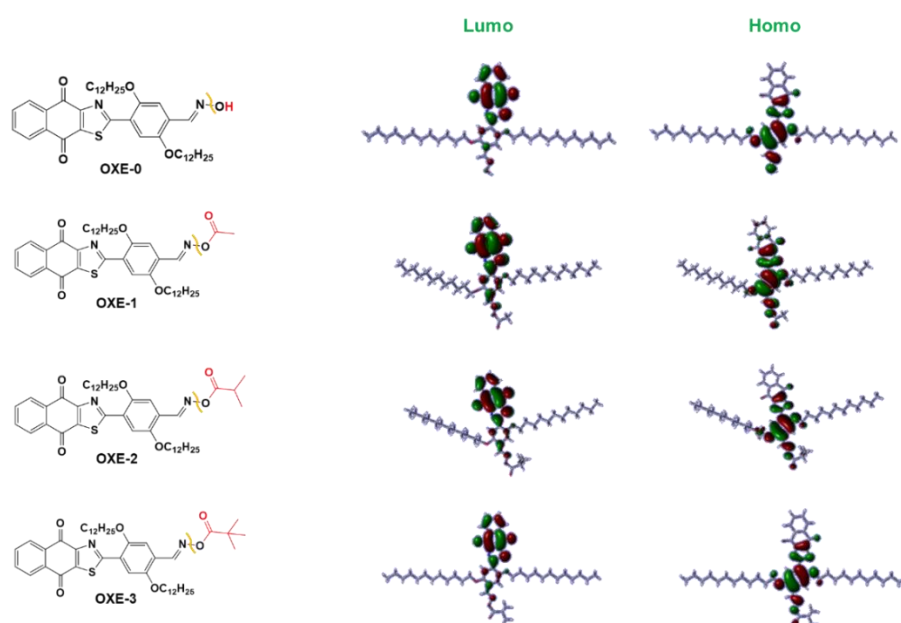


Figure 17. Contour plots of the HOMO and LUMO energy levels of OXE-1-OXE-3. Reproduced with permission of Ref. [214]

As a result of this redshift, OXE-1-OXE-8 were tested at 405 and 450 nm contrarily to the previous imidazole derivatives C1-C9 that were tested at short irradiation wavelengths, namely 365, 385 and 405 nm. Investigation of the bond dissociation energy (BDE) of OXE-1-OXE-9 by theoretical calculations revealed the BDE to around 43-45 kcal/mol (See Table 10).

For comparison, slightly higher BDEs were determined for the C1-C9 series, with values ranging between 48 and 49 kcal/mol (See Table 11). Irrespective of the series, the photocleavage of the N-O bond was determined as being more favorable from the singlet excited state than from the triplet states, with negative $\Delta H_{\text{Cleavage } S1}$ values (See Tables 10 and 11).

Table 10. Bond dissociation energy (BDE) of the N-O bond, energy of the singlet excited state (E_{S1}), energy of the triplet excited state (E_T), enthalpy of cleavage from the singlet or the triplet excited state ($\Delta H_{\text{Cleavage } S1}$ and $\Delta H_{\text{Cleavage } T1}$) of different OXEs.

PI	N-O BDE (kcal.mol ⁻¹)	E_{S1} (kcal.mol ⁻¹)	$\Delta H_{\text{Cleavage } S1}$ (kcal.mol ⁻¹)	E_T (kcal.mol ⁻¹)	$\Delta H_{\text{Cleavage } T1}$ (kcal.mol ⁻¹)
OXE-0	66.5	59.6	6.9	43.7	22.8
OXE-1	51.0	/	/	39.2	11.8
OXE-2	43.5	/	/	41.5	2.0
OXE-3	43.9	/	/	43.4	0.5
OXE-4	39.5	/	/	38.9	0.6
OXE-5	43.2	/	/	41.4	1.8
OXE-6	45.2	59.9	-14.7	42.7	2.5
OXE-7	43.3	60.2	-16.9	41.4	1.9
OXE-8	43.2	61.0	-17.8	42.6	0.6

Table 11. Bond dissociation energy (BDE) of the N-O bond, Energy of the singlet excited state (E_{S1}), Energy of the triplet excited state (E_T), Enthalpy of cleavage from the singlet or the triplet excited state ($\Delta H_{\text{Cleavage } S1}$ and $\Delta H_{\text{Cleavage } T1}$) of different OXEs

PI	BDE (kcal/mol)	E_{S1} (kcal/mol)	$\Delta H_{\text{cleavage}S1}$ (kcal/mol)	E_{T1} (kcal/mol)	$\Delta H_{\text{cleavage}T1}$ (kcal/mol)
C1	49.53	66.88	-17.35	48.46	1.07
C2	48.08	69.88	-21.8	48.48	-0.4
C3	49.19	64.58	-15.39	48.48	0.71
C4	48.59	63.19	-14.6	48.48	0.11
C5	48.35	63.88	-15.53	48.38	-0.03
C6	49.12	61.81	-12.69	48.47	0.65
C7	48.11	63.65	-15.54	48.25	-0.14
C8	47.22	68.49	-21.27	49.64	-2.42
C9	45.74	68.72	-22.98	48.54	-2.8

Considering that OXE-1-OXE-8 are oxime esters, these structures were first tested as monocomponent photoinitiators, at low photoinitiator content (0.1 and 0.05 wt%), in thick films and upon excitation at 405 and 450 nm (See Table 12). Noticeably, similar monomer

conversions were obtained at 0.1 and 0.05 wt% in thick samples evidencing the interest of these structures. Only a slight improvement of the monomer conversion was detected at 450 nm at 0.05 wt%, resulting from a higher transparency of the resins. As observed for the C1-C9 series, higher TMPTA double bond conversions were obtained with all oxime esters bearing aliphatic groups on the oxime ester side. Thus, if a TMPTA double bond conversion of 41% was obtained with OXE-2, this value was reduced to 22% with OXE-6. Comparisons of the monomer conversions with that obtained with two references photoinitiators (ITX, TPO) revealed the new structures to be less efficient at 405 nm. Conversely, at 450 nm, OXE-1-OXE-8 were still active, contrarily to ITX and TPO that do not absorb at this wavelength. However, due to lower molar extinction coefficients at 450 nm, a reduction of the TMPTA double bond conversions could be determined. For comparison, in the same conditions (405 nm, 0.1 wt%), the previous C1-C9 series could furnish higher TMPTA double bond conversions, despite less favorable absorption properties at this wavelength (See Table 6).

Table 12. Final monomer conversions (FCs) determined during the FRP of TMPTA in thick samples upon excitation at 405 and 450 nm after 400 s of irradiation

PI	405 nm		450 nm	
	0.1 wt%	0.05 wt%	0.1 wt%	0.05 wt%
	FC (%)	FC (%)	FC (%)	FC (%)
OXE-0	1	0.7	2	2
OXE-1	37	41	26	26
OXE-2	41	40	28	33
OXE-3	32	37	24	33
OXE-4	36	30	4	2
OXE-5	30	33	5	12
OXE-6	22	22	3	3
OXE-7	23	24	2	3
OXE-8	31	34	10	27
ITX	58	54	-	-
TPO	74	68	-	-

OXE-1-OXE-9 were also tested in two-component systems in combination with EDB and Iod. In this case, the most significant enhancement of the TMPTA double bond conversion was obtained with the two-component OXE/EDB systems. Thus, the TMPTA double bond conversion increased from 37 to 44 and finally 64% using OXE-1 alone, the two-component OXE-1/Iod system and the OXE-1/EDB combination. A further improvement could be obtained by using a three-component OXE-1/Iod/EDB system, peaking at 73% after 400 s of irradiation (See Table 13).

Table 13. TMPTA double bond conversions obtained at 405 nm with different two-component OXE/Iod and OXE/EDB systems. For the additive, the concentration was set to 0.1 wt%.

PI	Iod		EDB		Iod/EDB
	0.1 wt%	0.05 wt%	0.1 wt%	0.05 wt%	0.1 wt%
	FC (%)	FC (%)	FC (%)	FC (%)	FC (%)
OXE-0	0.9	2	48	48	57
OXE-1	44	52	64	67	73
OXE-2	26	50	62	68	70
OXE-3	55	49	62	69	73
OXE-4	39	41	62	67	72
OXE-5	42	45	63	63	72
OXE-6	49	38	56	60	65
OXE-7	33	32	60	63	68
OXE-8	9	46	60	66	63
ITX	63	71	76	71	78

Considering the high TMPTA double bond conversions that could be obtained with the three-component OXE/Iod/EDB systems upon excitation at 405 nm, their abilities to initiate polymerization processes under sunlight was examined. Contrarily to the artificial light that exhibits a narrow emission, the emission spectrum of Sun is broad. Parallel to this, light intensity of Sun is considerably lowered compared to that of artificial light sources, what can adversely affect the polymerization efficiency.[43,217] When tested under sunlight, photoinitiating systems based on OXE-1, OXE-2 and OXE-3 furnished a conversion of ca 40% within 5 min. of exposure, evidencing the reactivity of these systems. After 40 min. of irradiation, this conversion could increase up to 50%. Noticeably, OXE-4 and OXE-8 could furnish comparable monomer conversions (50% TMPTA double bond conversion after 40 min.) and these conversions are remarkable, considering their low reactivities under artificial light (See Figure 18). This is directly related to the broad emission spectrum of Sun enabling to better excite the dyes.

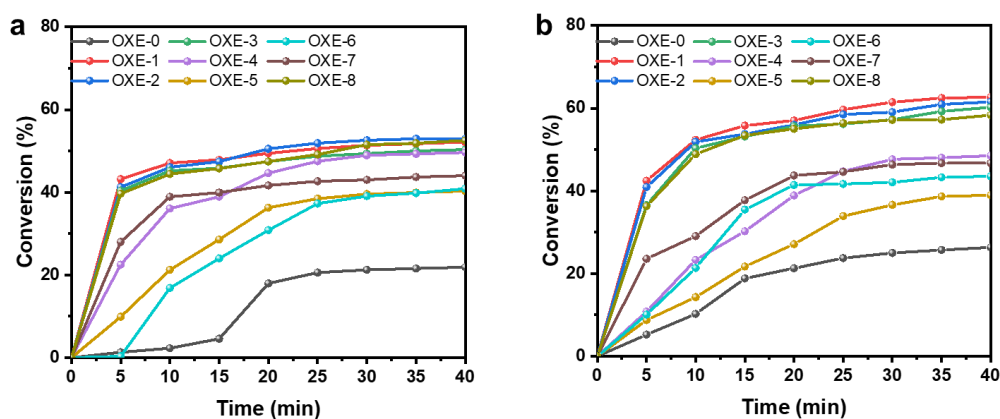


Figure 18. Sunlight-initiated photopolymerization of thick TMPTA samples using different three-component OXE/Iod/EDB (0.05%/0.1%/0.1% w/w/w) photoinitiating systems. Reproduced with permission of Ref. [214]

3.2. Type II photoinitiators

The design of solar photoinitiators is an active research field, considering the numerous outdoor applications of photopolymerization.[38–44,218–221] If various derivatives of 2-phenyl-1*H*-naphtho[2,3-*d*]imidazole-4,9-dione capable to act as Type I photoinitiators and activable under sunlight have been designed and synthesized, Type II photoinitiators have also been proposed, still with aim at developing solar photoinitiators. A series of fifteen dyes B1-B15 was proposed in 2024 by Lalevée and coworkers (See Figure 19).[47] The synthesis of the different dyes was straightforward, using 2-aminonaphthalene-1,4-dione RP1 as a common reagent (See Scheme 8).[215,222–225] By using the appropriate aldehyde ALD1-ALD15 in the presence of S₈ and NaHCO₃, B1-B15 could be obtained with reaction yields ranging from 65% for B13 up to 92% for B10 (See Table 14). For all these structures, a E-factor higher than 200 could be determined,[183,184] consistent with values determined for products prepared in fine and pharmaceutical chemistry. Examination of the optical properties of B1-B15 in dichloromethane revealed their absorption maxima to be strongly influenced by the electron withdrawing ability of the aldehyde used to prepare the different dyes. As shown in Figure 20 and in Table 15, the different dyes could be divided in two groups that later demonstrated severe differences of polymerization efficiency. Thus, B1, B2, B3, B10, and B11 exhibited absorption maxima located at 420, 400, 410, 410, and 400 nm, respectively i.e. the 400-420 nm range and proved to be highly reactive structures in photopolymerization. Conversely, B5, B7-B9, and B13-B15 strongly absorbs in the 450-600 nm range and only showed a poor photoinitiation ability. Comparisons with the absorption properties of the imidazole analogues Dye1-Dye10 revealed a blueshift of the absorption maxima by ca 10 nm by replacing the imidazole ring by a thiazole ring. Thus, if an absorption maximum located at 410 nm was determined for Dye 3, this value shifted to 400 nm for its analogue B2. These results can be assigned to the higher electron-donating ability of the thiazole ring compared to the imidazole ring, reducing the electron-accepting ability of the naphthoquinone moiety (See Tables 8 and 15).

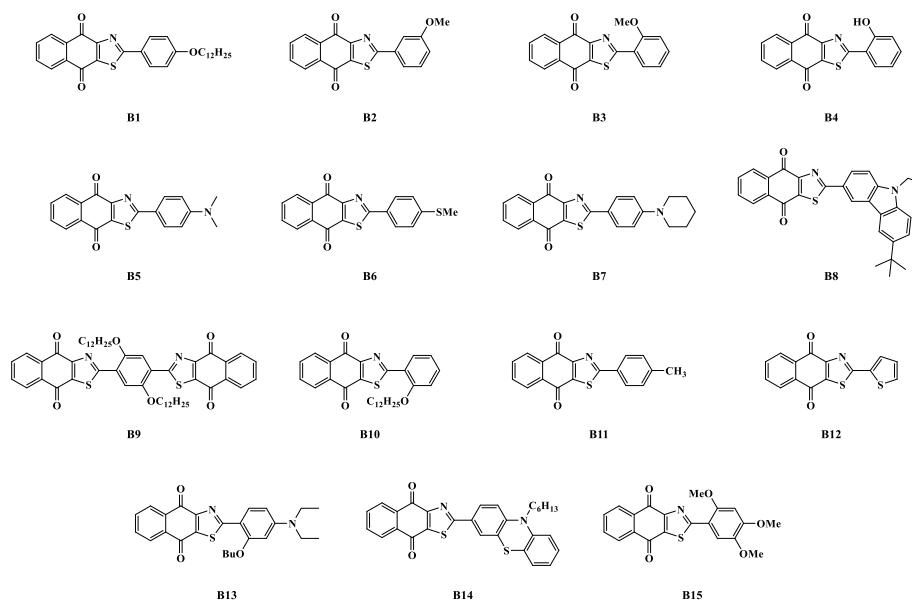
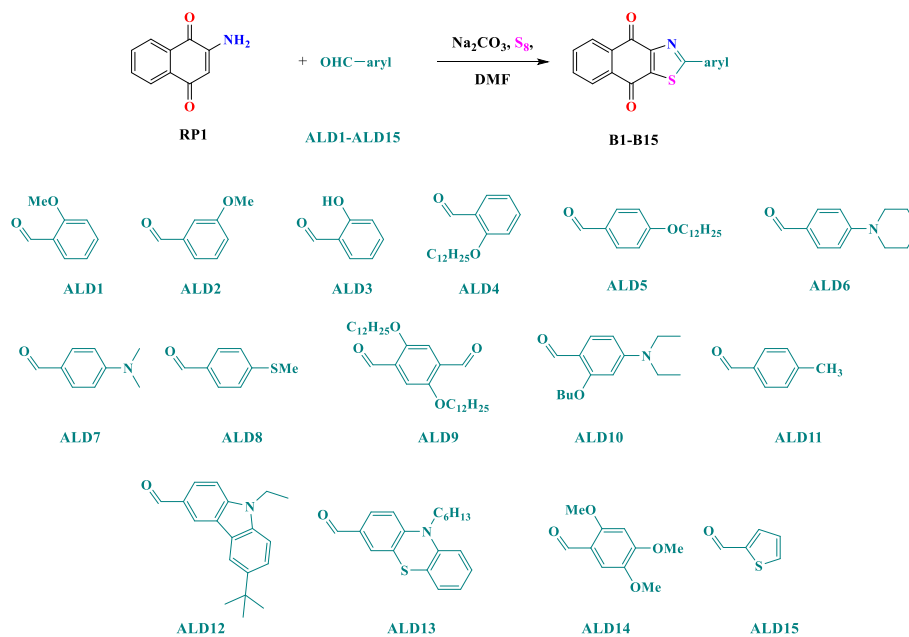


Figure 19. Structures of B1-B15 investigated by Lalevée and coworkers.



Scheme 8. Synthetic route to B1-B15.

Table 14. Reaction yields obtained during the synthesis of B1-B16.

Compounds	B1	B2	B3	B4	B5	B6
Reaction yield (%)	81	77	89	80	67	88
Compounds	B7	B8	B9	B10	B11	B12
Reaction yield (%)	88	91	58	92	81	88
Compounds	B13	B14	B15			
Reaction yield (%)	65	85	85			

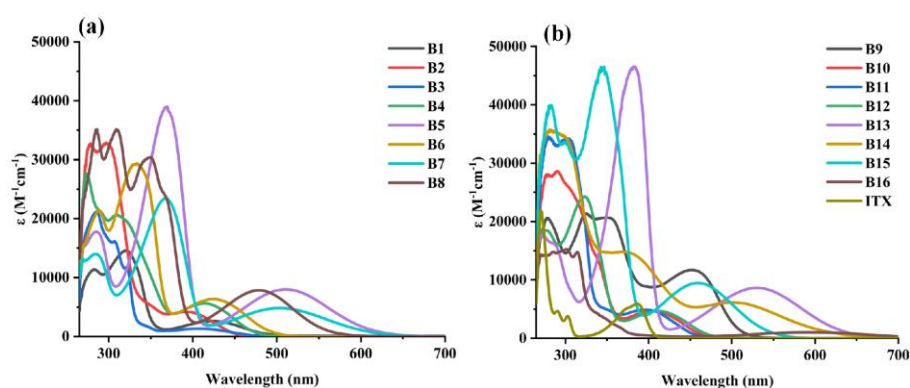


Figure 20. Absorption spectra of (a) B1-B8, (b) B9-B15 and ITX in dichloromethane. Reproduced with permission of Ref. [47]

Table 15. Light absorption characteristics of the dyes

PIs	λ_{\max} (nm)	ϵ_{\max} ($M^{-1}.cm^{-1}$)	ϵ_{405} ($M^{-1}.cm^{-1}$)	moiety
B1	420	2610	2310	4-dodecyloxyphenyl
B2	400	4170	3870	3-methoxyphenyl
B3	410	1320	1320	2-methoxyphenyl
B4	410	5600	5410	2-hydroxyphenyl
B5	510	7990	4110	4-dimethylaminophenyl
B6	430	6340	5630	4-methylthiophenyl
B7	510	4810	4570	4-piperidinylphenyl
B8	480	7830	2400	<i>tert</i> -butyl-(<i>N</i> -ethyl)carbazolyl
B9	450	11690	8760	naphthothiazolodione- <i>bis</i> (dodecyloxy)phenylene
B10	410	4690	4690	2-dodecyloxyphenyl
B11	400	4920	4730	<i>p</i> -tolyl
B12	410	4660	4570	thiophenyl
B13	530	8630	12120	2-butoxy-4-(diethylamino)phenyl
B14	500	6130	11240	<i>N</i> -hexyl-phenothiazinyl
B15	460	9460	4530	2,4,5-trimethoxyphenyl
ITX	390	5890	1000	

As anticipated, B1-B15 were unable to initiate any polymerization processes without additives such as Iod or EDB at 405 nm. When introduced in two-component dye/Iod and dye/EDB systems, an optimal concentration of 0.1 wt% was determined for the polymerization experiments. Noticeably, B1 furnished in the best TMPTA double bond conversion in thick sample (72%) what could be slightly improved in thin films (77%). Surprisingly, B2, B3, B10 and B11 that could furnish a TMPTA double bond conversion ranging between 62 and 70% in

thick films were less efficient in thin samples (between 43 and 53%, see Table 16). Finally, B4, B6 and B16 that were moderate photoinitiators in thick samples (56, 55 and 48% respectively) proved to be exceptional photoinitiators in thin samples (89, 88 and 90% respectively). Interestingly, all dyes could also promote the FRP of TMPTA with the two-component dye/Iod system so that the photoinitiating ability of the three-component dye/Iod/EDB systems was examined. Thus, for B3, the TMPTA double bond conversion in thick films increased from 65% with the two-component dye/EDB (0.1%/1% w/w) system up to 91% for the three-component dye/Iod/EDB (0.1%/1%/1% w/w/w) system (See Figure 21). This value is slightly higher than that obtained with ITX (87%). Considering that the best monomer conversions were obtained with B1, B2, B3, B10 and B11 in thick films, these structures were then tested as solar photoinitiators.

Table 16. FCs of TMPTA for thick and thin samples using the two-component dye/EDB (0.1%/1% w/w) systems upon excitation at 405 nm.

Thick sample		Thin sample	
Dye/EDB (0.1%/1% w/w)	FCs (%)	Dye/EDB (0.1%/1% w/w)	FCs (%)
ITX	82	ITX	-
B1	72	B1	77
B10	70	B10	51
B3	65	B3	53
B2	62	B2	43
B11	62	B11	48
B12	57	B12	-
B4	56	B4	89
B6	55	B6	47
B9	49	B9	88
B16	48	B16	90

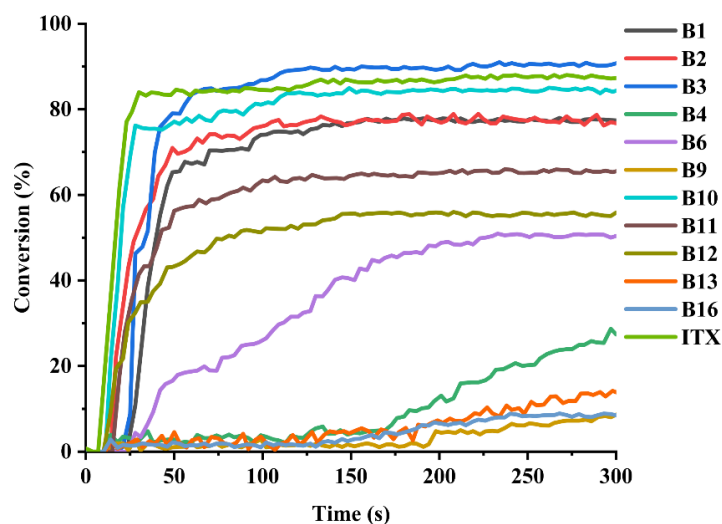


Figure 21. TMPTA double bond conversions obtained with the three-component dye/Iod/EDB (0.1%/1%/1% w/w/w) systems upon excitation at 405 nm of thick samples. Reproduced with permission of Ref. [47]

Interestingly, in the case of B10, a TMPTA double bond conversion higher than 50% could be obtained within 10 s, evidencing the high reactivity of this structure. Even if B1, B2, B3 and B11 were slightly less reactive than B10, a complete curing of the resins could be obtained after 60 s of sunlight exposure (See Figure 22). In turn, this family of 2-phenylnaphtho[2,3-*d*]thiazole-4,9-diones is exceptional in terms of reactivity. Indeed, as shown in Table 17, previous dyes reported in the literature could furnish higher TMPTA double bond conversions than the 2-phenylnaphtho[2,3-*d*]thiazole-4,9-dione derivatives,[44,226,227] but after long irradiation time (around 30 min.)

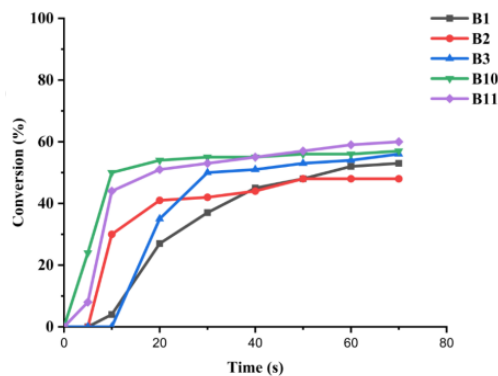
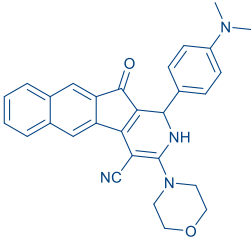
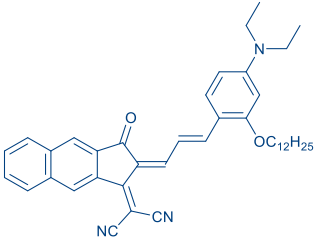
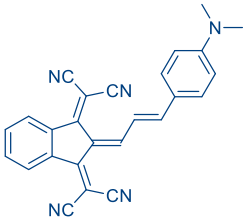
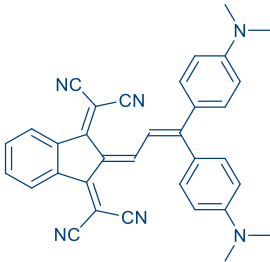


Figure 22. TMPTA double bond conversions using the three-component dye/Iod/EDB (0.1%/1%/1% w/w/w) systems under sunlight and under air. Reproduced with permission of Ref. [47]

Table 17. TMPTA double bond conversions obtained at 405 nm and sunlight (30 min) using three-component photoinitiating dye/Iod/EDB (0.1%/2%/2% w/w/w) systems.

	Push-pull dyes	Absorption properties	Final Acrylate function conversion
Dye8 [226]		$\lambda_{\max} = 491 \text{ nm}$ $\epsilon_{\max} = 5330 \text{ M}^{-1} \cdot \text{cm}^{-1}$ $\epsilon_{405\text{nm}} = 3340 \text{ M}^{-1} \cdot \text{cm}^{-1}$	~91% (LED@405 nm, I = 110 mW.cm ⁻² , 400 s); ~88% (sunlight, 30 min)
CP7 [227]		$\lambda_{\max} = 689 \text{ nm}$ $\epsilon_{\max} = 113870 \text{ M}^{-1} \cdot \text{cm}^{-1}$ $\epsilon_{405\text{nm}} = 13640 \text{ M}^{-1} \cdot \text{cm}^{-1}$	~97% (LED@405 nm, I = 30 mW.cm ⁻² , 400 s); ~93% (sunlight, 30 min)
CP9 [227]		$\lambda_{\max} = 627 \text{ nm}$ $\epsilon_{\max} = 51700 \text{ M}^{-1} \cdot \text{cm}^{-1}$ $\epsilon_{405\text{nm}} = 4610 \text{ M}^{-1} \cdot \text{cm}^{-1}$	~98% (LED@405 nm, I = 30 mW.cm ⁻² , 400 s); ~91% (sunlight, 30 min)
CP11 [227]		$\lambda_{\max} = 671 \text{ nm}$ $\epsilon_{\max} = 47770 \text{ M}^{-1} \cdot \text{cm}^{-1}$ $\epsilon_{405\text{nm}} = 6560 \text{ M}^{-1} \cdot \text{cm}^{-1}$	~99% (LED@405 nm, I = 30 mW.cm ⁻² , 400 s); ~92% (sunlight, 30 min)

Conclusion

In the search for new photoinitiators that could enable to polymerize monomers in greener synthetic conditions than that currently used, 2-phenyl-1*H*-naphtho[2,3-*d*]imidazole-4,9-dione and 2-phenyl-naphtho[2,3-*d*]thiazole-4,9-dione have been identified as promising scaffold for design sunlight photoinitiators. Besides, these different works have clearly evidenced that in type I photoinitiators, the distance between the photocleavable group and the chromophore is an important parameter to consider in order to design efficient photoinitiators. By increasing the distance, the cleavage efficiency is reduced. Comparison between the two families of chromophores have evidenced that 2-phenyl-naphtho[2,3-*d*]thiazole-4,9-dione was a better scaffold due to the absence of the acidic NH proton that is present in 2-phenyl-1*H*-naphtho[2,3-*d*]imidazole-4,9-dione that was adversely affecting the solubility in organic solvents but also in resins.

In order to polymerize in more environmentally friendly conditions, future works will consist in designing water-soluble photoinitiators, enabling to polymerize hydrogels. Parallel

to this, visible light photoinitiators are still the focus of criticisms, especially with regards to their strong colours which is important since it enables these structures to harvest visible light but adversely impact the colour of the final polymers by providing an undesired colour. The development of photobleachable structures will be necessary to expand the scope of applications of visible light photopolymerization. The development of such innovative structures will be obtained at the price of an extensive synthetic works.

Nowadays, polymer recycling is an active research field, with regards to the polymer waster produced daily. The development of photoinitiators that could be used as photoinitiators of depolymerization after polymer use should be developed in the Future.

References

- [1] J. Lalevée, H. Mokbel, J.-P. Fouassier, Recent Developments of Versatile Photoinitiating Systems for Cationic Ring Opening Polymerization Operating at Any Wavelengths and under Low Light Intensity Sources, *Molecules* 20 (2015) 7201–7221. <https://doi.org/10.3390/molecules20047201>.
- [2] M.A. Tehfe, F. Louradour, J. Lalevée, J.-P. Fouassier, Photopolymerization Reactions: On the Way to a Green and Sustainable Chemistry, *Applied Sciences* 3 (2013) 490–514. <https://doi.org/10.3390/app3020490>.
- [3] Y. Zhang, Y. Xu, A. Simon-Masseron, J. Lalevée, Radical photoinitiation with LEDs and applications in the 3D printing of composites, *Chem. Soc. Rev.* 50 (2021) 3824–3841. <https://doi.org/10.1039/D0CS01411G>.
- [4] F. Dumur, Recent Advances on Visible Light Metal-Based Photocatalysts for Polymerization under Low Light Intensity, *Catalysts* 9 (2019) 736. <https://doi.org/10.3390/catal9090736>.
- [5] C. Pigot, G. Noirbent, D. Brunel, F. Dumur, Recent advances on push–pull organic dyes as visible light photoinitiators of polymerization, *European Polymer Journal* 133 (2020) 109797. <https://doi.org/10.1016/j.eurpolymj.2020.109797>.
- [6] W. Tomal, J. Ortyl, Water-Soluble Photoinitiators in Biomedical Applications, *Polymers* 12 (2020) 1073. <https://doi.org/10.3390/polym12051073>.
- [7] N. Corrigan, J. Yeow, P. Judzewitsch, J. Xu, C. Boyer, Seeing the Light: Advancing Materials Chemistry through Photopolymerization, *Angewandte Chemie International Edition* 58 (2019) 5170–5189. <https://doi.org/10.1002/anie.201805473>.
- [8] A. Banerji, K. Jin, K. Liu, M.K. Mahanthappa, C.J. Ellison, Cross-Linked Nonwoven Fibers by Room-Temperature Cure Blowing and in Situ Photopolymerization, *Macromolecules* 52 (2019) 6662–6672. <https://doi.org/10.1021/acs.macromol.9b01002>.
- [9] G. Yilmaz, Y. Yagci, Light-induced step-growth polymerization, *Progress in Polymer Science* 100 (2020) 101178. <https://doi.org/10.1016/j.progpolymsci.2019.101178>.
- [10] M. Layani, X. Wang, S. Magdassi, Novel Materials for 3D Printing by Photopolymerization, *Advanced Materials* 30 (2018) 1706344. <https://doi.org/10.1002/adma.201706344>.
- [11] C. Dietlin, S. Schweizer, P. Xiao, J. Zhang, F. Morlet-Savary, B. Graff, J.-P. Fouassier, J. Lalevée, Photopolymerization upon LEDs: new photoinitiating systems and strategies, *Polym. Chem.* 6 (2015) 3895–3912. <https://doi.org/10.1039/C5PY00258C>.

- [12] S. Shanmugam, J. Xu, C. Boyer, Photocontrolled Living Polymerization Systems with Reversible Deactivations through Electron and Energy Transfer, *Macromolecular Rapid Communications* 38 (2017) 1700143. <https://doi.org/10.1002/marc.201700143>.
- [13] S.M. Müller, S. Schlögl, T. Wiesner, M. Haas, T. Griesser, Recent Advances in Type I Photoinitiators for Visible Light Induced Photopolymerization, *ChemPhotoChem* 6 (2022) e202200091. <https://doi.org/10.1002/cptc.202200091>.
- [14] C. Förster, A. Andrieu-Brunsen, Recent developments in visible light induced polymerization towards its application to nanopores, *Chem. Commun.* 59 (2023) 1554–1568. <https://doi.org/10.1039/D2CC06595A>.
- [15] R. Canterel, J. Lalevée, E. Bourgeat-Lami, E. Lacôte, M. Lansalot, Visible-Light Initiated Dispersion Photopolymerization of Styrene, *Angewandte Chemie International Edition* 62 (2023) e202309674. <https://doi.org/10.1002/anie.202309674>.
- [16] X. Dong, P. Hu, G. Zhu, Z. Li, R. Liu, X. Liu, Thioxanthone acetic acid ammonium salts: highly efficient photobase generators based on photodecarboxylation, *RSC Adv.* 5 (2015) 53342–53348. <https://doi.org/10.1039/C5RA09314G>.
- [17] F. Dumur, Recent advances on pyrene-based photoinitiators of polymerization, *European Polymer Journal* 126 (2020) 109564. <https://doi.org/10.1016/j.eurpolymj.2020.109564>.
- [18] J. Zhang, N. Zivic, F. Dumur, P. Xiao, B. Graff, J.P. Fouassier, D. Gigmes, J. Lalevée, N-[2-(Dimethylamino)ethyl]-1,8-naphthalimide derivatives as photoinitiators under LEDs, *Polym. Chem.* 9 (2018) 994–1003. <https://doi.org/10.1039/C8PY00055G>.
- [19] M.-A. Tehfe, M. Lepeltier, F. Dumur, D. Gigmes, J.-P. Fouassier, J. Lalevée, Structural Effects in the Iridium Complex Series: Photoredox Catalysis and Photoinitiation of Polymerization Reactions under Visible Lights, *Macromolecular Chemistry and Physics* 218 (2017) 1700192. <https://doi.org/10.1002/macp.201700192>.
- [20] P. Xiao, J. Zhang, D. Campolo, F. Dumur, D. Gigmes, J.P. Fouassier, J. Lalevée, Copper and iron complexes as visible-light-sensitive photoinitiators of polymerization, *Journal of Polymer Science Part A: Polymer Chemistry* 53 (2015) 2673–2684. <https://doi.org/10.1002/pola.27762>.
- [21] L. Pezzana, G. Melilli, N. Guigo, N. Sbirrazzuoli, M. Sangermano, Photopolymerization of furan-based monomers: Exploiting UV-light for a new age of green polymers, *Reactive and Functional Polymers* 185 (2023) 105540. <https://doi.org/10.1016/j.reactfunctpolym.2023.105540>.
- [22] A. Balcerak, J. Kabatc, Z. Czech, M. Nowak, K. Mozelewska, High-Performance UV-Vis Light Induces Radical Photopolymerization Using Novel 2-Aminobenzothiazole-Based Photosensitizers, *Materials* 14 (2021). <https://doi.org/10.3390/ma14247814>.
- [23] T.T.H. Luu, Z. Jia, A. Kanaev, L. Museur, Effect of Light Intensity on the Free-Radical Photopolymerization Kinetics of 2-Hydroxyethyl Methacrylate: Experiments and Simulations, *J. Phys. Chem. B* 124 (2020) 6857–6866. <https://doi.org/10.1021/acs.jpcc.0c03140>.
- [24] J. Bennett, Measuring UV curing parameters of commercial photopolymers used in additive manufacturing, *Additive Manufacturing* 18 (2017) 203–212. <https://doi.org/10.1016/j.addma.2017.10.009>.
- [25] R. Anastasio, W. Peerbooms, R. Cardinaels, L.C.A. van Breemen, Characterization of Ultraviolet-Cured Methacrylate Networks: From Photopolymerization to Ultimate Mechanical Properties, *Macromolecules* 52 (2019) 9220–9231. <https://doi.org/10.1021/acs.macromol.9b01439>.

- [26] E. Hola, M. Topa, A. Chachaj-Brekiesz, M. Pilch, P. Fiedor, M. Galek, J. Ortyl, New, highly versatile bimolecular photoinitiating systems for free-radical, cationic and thiol-ene photopolymerization processes under low light intensity UV and visible LEDs for 3D printing application, *RSC Adv.* 10 (2020) 7509–7522. <https://doi.org/10.1039/C9RA10212D>.
- [27] J. Shao, Y. Huang, Q. Fan, Visible light initiating systems for photopolymerization: status, development and challenges, *Polym. Chem.* 5 (2014) 4195–4210. <https://doi.org/10.1039/C4PY00072B>.
- [28] H.K. Park, M. Shin, B. Kim, J.W. Park, H. Lee, A visible light-curable yet visible wavelength-transparent resin for stereolithography 3D printing, *NPG Asia Mater* 10 (2018) 82–89. <https://doi.org/10.1038/s41427-018-0021-x>.
- [29] F. Yoshino, A. Yoshida, Effects of blue-light irradiation during dental treatment, *Jpn Dent Sci Rev* 54 (2018) 160–168. <https://doi.org/10.1016/j.jdsr.2018.06.002>.
- [30] P. Garra, C. Dietlin, F. Morlet-Savary, F. Dumur, D. Gignes, J.-P. Fouassier, J. Lalevée, Redox two-component initiated free radical and cationic polymerizations: Concepts, reactions and applications, *Progress in Polymer Science* 94 (2019) 33–56. <https://doi.org/10.1016/j.progpolymsci.2019.04.003>.
- [31] J.P. Fouassier, X. Allonas, D. Burget, Photopolymerization reactions under visible lights: principle, mechanisms and examples of applications, *Progress in Organic Coatings* 47 (2003) 16–36. [https://doi.org/10.1016/S0300-9440\(03\)00011-0](https://doi.org/10.1016/S0300-9440(03)00011-0).
- [32] P. Fiedor, M. Pilch, P. Szymaszek, A. Chachaj-Brekiesz, M. Galek, J. Ortyl, Photochemical Study of a New Bimolecular Photoinitiating System for Vat Photopolymerization 3D Printing Techniques under Visible Light, *Catalysts* 10 (2020) 284. <https://doi.org/10.3390/catal10030284>.
- [33] C. Mendes-Felipe, J. Oliveira, I. Etxebarria, J.L. Vilas-Vilela, S. Lanceros-Mendez, State-of-the-Art and Future Challenges of UV Curable Polymer-Based Smart Materials for Printing Technologies, *Advanced Materials Technologies* 4 (2019) 1800618. <https://doi.org/10.1002/admt.201800618>.
- [34] V. Shukla, M. Bajpai, D.K. Singh, M. Singh, R. Shukla, Review of basic chemistry of UV-curing technology, *Pigment & Resin Technology* 33 (2004) 272–279. <https://doi.org/10.1108/03699420410560461>.
- [35] M. Chen, M. Zhong, J.A. Johnson, Light-Controlled Radical Polymerization: Mechanisms, Methods, and Applications, *Chem. Rev.* 116 (2016) 10167–10211. <https://doi.org/10.1021/acs.chemrev.5b00671>.
- [36] J.V. Crivello, E. Reichmanis, Photopolymer Materials and Processes for Advanced Technologies, *Chem. Mater.* 26 (2014) 533–548. <https://doi.org/10.1021/cm402262g>.
- [37] A.H. Bonardi, F. Dumur, T.M. Grant, G. Noirbent, D. Gignes, B.H. Lessard, J.-P. Fouassier, J. Lalevée, High Performance Near-Infrared (NIR) Photoinitiating Systems Operating under Low Light Intensity and in the Presence of Oxygen, *Macromolecules* 51 (2018) 1314–1324. <https://doi.org/10.1021/acs.macromol.8b00051>.
- [38] M. Ciftci, M.A. Tasdelen, Y. Yagci, Sunlight induced atom transfer radical polymerization by using dimanganese decacarbonyl, *Polym. Chem.* 5 (2014) 600–606. <https://doi.org/10.1039/C3PY01009K>.
- [39] D. Konkolewicz, K. Schröder, J. Buback, S. Bernhard, K. Matyjaszewski, Visible Light and Sunlight Photoinduced ATRP with ppm of Cu Catalyst, *ACS Macro Lett.* 1 (2012) 1219–1223. <https://doi.org/10.1021/mz300457e>.

- [40] J. Lalevée, J.P. Fouassier, Recent advances in sunlight induced polymerization: role of new photoinitiating systems based on the silyl radical chemistry, *Polym. Chem.* 2 (2011) 1107–1113. <https://doi.org/10.1039/C1PY00073J>.
- [41] K. Sun, H. Chen, Y. Zhang, F. Morlet-Savary, B. Graff, P. Xiao, F. Dumur, J. Lalevée, High-performance sunlight induced polymerization using novel push-pull dyes with high light absorption properties, *European Polymer Journal* 151 (2021) 110410. <https://doi.org/10.1016/j.eurpolymj.2021.110410>.
- [42] M.-A. Tehfe, J. Lalevée, D. Gigmes, J.P. Fouassier, Green Chemistry: Sunlight-Induced Cationic Polymerization of Renewable Epoxy Monomers Under Air, *Macromolecules* 43 (2010) 1364–1370. <https://doi.org/10.1021/ma9025702>.
- [43] N.C.S. Tan, I. Djordjevic, J.A. Malley, A.L.Q. Kwang, S. Ikhwan, I. Šolić, J. Singh, G. Wicaksono, S. Lim, T.W.J. Steele, Sunlight activated film forming adhesive polymers, *Materials Science and Engineering: C* 127 (2021) 112240. <https://doi.org/10.1016/j.msec.2021.112240>.
- [44] F. Dumur, Recent Advances on Photoinitiating Systems Designed for Solar Photocrosslinking Polymerization Reactions, *European Polymer Journal* 189 (2023) 111988. <https://doi.org/10.1016/j.eurpolymj.2023.111988>.
- [45] J. Feng, T. Gao, F. Morlet-Savary, M. Schmitt, C. Dietlin, J. Zhang, P. Xiao, F. Dumur, J. Lalevée, Sunlight-driven photoinitiating systems for photopolymerization and application in direct laser writing, *Polym. Chem.* 15 (2024) 2899–2912. <https://doi.org/10.1039/D4PY00558A>.
- [46] Y. Zhang, B. Song, Z. Liu, A. Noon, C. Dietlin, F. Morlet-Savary, M. Schmitt, D. Gigmes, F. Dumur, J. Lalevée, High Photoinitiating Efficiency of Benzothioxanthene-Based Oxime Esters in Photopolymerization via Photocleavage and/or Single Electron Transfer under Visible Light and Sunlight, *Angewandte Chemie International Edition* n/a (2024) e202405337. <https://doi.org/10.1002/anie.202405337>.
- [47] J. Feng, Y. Zhang, F. Morlet-Savary, M. Schmitt, J. Zhang, P. Xiao, F. Dumur, J. Lalevée, Ultrafast Sunlight-Induced Polymerization: Unveiling 2-Phenylnaphtho[2,3-d]Thiazole-4,9-dione as a Unique Scaffold for High-Speed and Precision 3D Printing, *Small* n/a (2024) 2400230. <https://doi.org/10.1002/smll.202400230>.
- [48] Y. Zhang, Z. Liu, T. Borjigin, B. Graff, F. Morlet-Savary, M. Schmitt, D. Gigmes, F. Dumur, J. Lalevée, Carbazole-fused coumarin based oxime esters (OXEs): efficient photoinitiators for sunlight driven free radical photopolymerization, *Green Chem.* 25 (2023) 6881–6891. <https://doi.org/10.1039/D3GC02004E>.
- [49] J. Zhang, D. Campolo, F. Dumur, P. Xiao, D. Gigmes, J.P. Fouassier, J. Lalevée, The carbazole-bound ferrocenium salt as a specific cationic photoinitiator upon near-UV and visible LEDs (365–405 nm), *Polym. Bull.* 73 (2016) 493–507. <https://doi.org/10.1007/s00289-015-1506-1>.
- [50] A. Al Mousawi, P. Garra, F. Dumur, T.-T. Bui, F. Goubard, J. Toufaily, T. Hamieh, B. Graff, D. Gigmes, J.P. Fouassier, J. Lalevée, Novel Carbazole Skeleton-Based Photoinitiators for LED Polymerization and LED Projector 3D Printing, *Molecules* 22 (2017) 2143. <https://doi.org/10.3390/molecules22122143>.
- [51] M. Abdallah, D. Magaldi, A. Hijazi, B. Graff, F. Dumur, J.-P. Fouassier, T.-T. Bui, F. Goubard, J. Lalevée, Development of new high-performance visible light photoinitiators based on carbazole scaffold and their applications in 3d printing and photocomposite synthesis, *Journal of Polymer Science Part A: Polymer Chemistry* 57 (2019) 2081–2092. <https://doi.org/10.1002/pola.29471>.

- [52] F. Dumur, Recent advances on carbazole-based photoinitiators of polymerization, *European Polymer Journal* 125 (2020) 109503. <https://doi.org/10.1016/j.eurpolymj.2020.109503>.
- [53] S. Telitel, F. Dumur, T. Faury, B. Graff, M.-A. Tehfe, D. Gigmes, J.-P. Fouassier, J. Lalevée, New core-pyrene π structure organophotocatalysts usable as highly efficient photoinitiators, *Beilstein J. Org. Chem.* 9 (2013) 877–890. <https://doi.org/10.3762/bjoc.9.101>.
- [54] N. Uchida, H. Nakano, T. Igarashi, T. Sakurai, Nonsalt 1-(arylmethoxy)pyrene photoinitiators capable of initiating cationic polymerization, *Journal of Applied Polymer Science* 131 (2014) 40510. <https://doi.org/10.1002/app.40510>.
- [55] A. Mishra, S. Daswal, 1-(Bromoacetyl)pyrene, a novel photoinitiator for the copolymerization of styrene and methylmethacrylate, *Radiation Physics and Chemistry* 75 (2006) 1093–1100. <https://doi.org/10.1016/j.radphyschem.2006.01.013>.
- [56] N. Zivic, M. Bouzrati-Zerrelli, S. Villotte, F. Morlet-Savary, C. Dietlin, F. Dumur, D. Gigmes, J.P. Fouassier, J. Lalevée, A novel naphthalimide scaffold based iodonium salt as a one-component photoacid/photoinitiator for cationic and radical polymerization under LED exposure, *Polym. Chem.* 7 (2016) 5873–5879. <https://doi.org/10.1039/C6PY01306F>.
- [57] G. Noirbent, F. Dumur, Recent advances on naphthalic anhydrides and 1,8-naphthalimide-based photoinitiators of polymerization, *European Polymer Journal* 132 (2020) 109702. <https://doi.org/10.1016/j.eurpolymj.2020.109702>.
- [58] F. Dumur, D. Bertin, D. Gigmes, Iridium (III) complexes as promising emitters for solid-state Light-Emitting Electrochemical Cells (LECs), *International Journal of Nanotechnology* 9 (2012) 377–395. <https://doi.org/10.1504/IJNT.2012.045343>.
- [59] F. Dumur, G. Nasr, G. Wantz, C.R. Mayer, E. Dumas, A. Guerlin, F. Miomandre, G. Clavier, D. Bertin, D. Gigmes, Cationic iridium complex for the design of soft salt-based phosphorescent OLEDs and color-tunable light-emitting electrochemical cells, *Organic Electronics* 12 (2011) 1683–1694. <https://doi.org/10.1016/j.orgel.2011.06.014>.
- [60] P. Xiao, F. Dumur, J. Zhang, D. Gigmes, J.P. Fouassier, J. Lalevée, Copper complexes: the effect of ligands on their photoinitiation efficiencies in radical polymerization reactions under visible light, *Polym. Chem.* 5 (2014) 6350–6357. <https://doi.org/10.1039/C4PY00925H>.
- [61] H. Mokbel, D. Anderson, R. Plenderleith, C. Dietlin, F. Morlet-Savary, F. Dumur, D. Gigmes, J.-P. Fouassier, J. Lalevée, Copper photoredox catalyst “G1”: a new high performance photoinitiator for near-UV and visible LEDs, *Polym. Chem.* 8 (2017) 5580–5592. <https://doi.org/10.1039/C7PY01016H>.
- [62] H. Mokbel, D. Anderson, R. Plenderleith, C. Dietlin, F. Morlet-Savary, F. Dumur, D. Gigmes, J.P. Fouassier, J. Lalevée, Simultaneous initiation of radical and cationic polymerization reactions using the “G1” copper complex as photoredox catalyst: Applications of free radical/cationic hybrid photopolymerization in the composites and 3D printing fields, *Progress in Organic Coatings* 132 (2019) 50–61. <https://doi.org/10.1016/j.porgcoat.2019.02.044>.
- [63] P. Garra, F. Dumur, D. Gigmes, A. Al Mousawi, F. Morlet-Savary, C. Dietlin, J.P. Fouassier, J. Lalevée, Copper (Photo)redox Catalyst for Radical Photopolymerization in Shadowed Areas and Access to Thick and Filled Samples, *Macromolecules* 50 (2017) 3761–3771. <https://doi.org/10.1021/acs.macromol.7b00622>.

- [64] G. Noirbent, F. Dumur, Recent Advances on Copper Complexes as Visible Light Photoinitiators and (Photo) Redox Initiators of Polymerization, *Catalysts* 10 (2020). <https://doi.org/10.3390/catal10090953>.
- [65] J. Zhang, D. Campolo, F. Dumur, P. Xiao, J.P. Fouassier, D. Gimes, J. Lalevée, Iron complexes as photoinitiators for radical and cationic polymerization through photoredox catalysis processes, *Journal of Polymer Science Part A: Polymer Chemistry* 53 (2015) 42–49. <https://doi.org/10.1002/pola.27435>.
- [66] F. Dumur, Recent advances on ferrocene-based photoinitiating systems, *European Polymer Journal* 147 (2021) 110328. <https://doi.org/10.1016/j.eurpolymj.2021.110328>.
- [67] F. Dumur, Recent advances on iron-based photoinitiators of polymerization, *European Polymer Journal* 139 (2020) 110026. <https://doi.org/10.1016/j.eurpolymj.2020.110026>.
- [68] H. Mokbel, F. Dumur, J. Lalevée, On demand NIR activated photopolyaddition reactions, *Polym. Chem.* 11 (2020) 4250–4259. <https://doi.org/10.1039/D0PY00639D>.
- [69] H. Mokbel, B. Graff, F. Dumur, J. Lalevée, NIR Sensitizer Operating under Long Wavelength (1064 nm) for Free Radical Photopolymerization Processes, *Macromolecular Rapid Communications* 41 (2020) 2000289. <https://doi.org/10.1002/marc.202000289>.
- [70] V. Launay, F. Dumur, D. Gimes, J. Lalevée, Near-infrared light for polymer re-shaping and re-processing applications, *Journal of Polymer Science* 59 (2021) 2193–2200. <https://doi.org/10.1002/pol.20210450>.
- [71] V. Launay, F. Dumur, L. Pieuchot, J. Lalevée, Safe near infrared light for fast polymers surface sterilization using organic heaters, *Mater. Chem. Front.* 6 (2022) 1172–1179. <https://doi.org/10.1039/D1QM01609A>.
- [72] V. Launay, R. Wolf, F. Dumur, J. Lalevée, Photothermal activation in the near infrared range for 4-dimensional printing using relevant organic dyes, *Additive Manufacturing* 58 (2022) 103031. <https://doi.org/10.1016/j.addma.2022.103031>.
- [73] L. Tang, J. Nie, X. Zhu, A high performance phenyl-free LED photoinitiator for cationic or hybrid photopolymerization and its application in LED cationic 3D printing, *Polym. Chem.* 11 (2020) 2855–2863. <https://doi.org/10.1039/D0PY00142B>.
- [74] S. Liu, Y. Zhang, K. Sun, B. Graff, P. Xiao, F. Dumur, J. Lalevée, Design of photoinitiating systems based on the chalcone-anthracene scaffold for LED cationic photopolymerization and application in 3D printing, *European Polymer Journal* 147 (2021) 110300. <https://doi.org/10.1016/j.eurpolymj.2021.110300>.
- [75] N. Giacoletto, F. Dumur, Recent Advances in bis-Chalcone-Based Photoinitiators of Polymerization: From Mechanistic Investigations to Applications, *Molecules* 26 (2021) 3192. <https://doi.org/10.3390/molecules26113192>.
- [76] M. Ibrahim-Ouali, F. Dumur, Recent Advances on Chalcone-based Photoinitiators of Polymerization, *European Polymer Journal* 158 (2021) 110688. <https://doi.org/10.1016/j.eurpolymj.2021.110688>.
- [77] K. Sun, Y. Xu, F. Dumur, F. Morlet-Savary, H. Chen, C. Dietlin, B. Graff, J. Lalevée, P. Xiao, In silico rational design by molecular modeling of new ketones as photoinitiators in three-component photoinitiating systems: application in 3D printing, *Polym. Chem.* 11 (2020) 2230–2242. <https://doi.org/10.1039/C9PY01874C>.
- [78] M.-A. Tehfe, F. Dumur, B. Graff, J.-L. Clément, D. Gimes, F. Morlet-Savary, J.-P. Fouassier, J. Lalevée, New Cleavable Photoinitiator Architecture with Huge Molar Extinction Coefficients for Polymerization in the 340–450 nm Range., *Macromolecules* 46 (2013) 736–746. <https://doi.org/10.1021/ma3024359>.

- [79] B. Jędrzejewska, B. Ośmiałowski, Difluoroboranyl derivatives as efficient panchromatic photoinitiators in radical polymerization reactions, *Polym. Bull.* 75 (2018) 3267–3281. <https://doi.org/10.1007/s00289-017-2201-1>.
- [80] A. Mau, G. Noirbent, C. Dietlin, B. Graff, D. Gigmes, F. Dumur, J. Lalevée, Panchromatic Copper Complexes for Visible Light Photopolymerization, *Photochem 1* (2021). <https://doi.org/10.3390/photochem1020010>.
- [81] M. Topa-Skwarczyńska, M. Galek, M. Jankowska, F. Morlet-Savary, B. Graff, J. Lalevée, R. Popielarz, J. Ortyl, Development of the first panchromatic BODIPY-based one-component iodonium salts for initiating the photopolymerization processes, *Polym. Chem.* 12 (2021) 6873–6893. <https://doi.org/10.1039/D1PY01263K>.
- [82] H. Tar, D. Sevinc Esen, M. Aydin, C. Ley, N. Arsu, X. Allonas, Panchromatic Type II Photoinitiator for Free Radical Polymerization Based on Thioxanthone Derivative, *Macromolecules* 46 (2013) 3266–3272. <https://doi.org/10.1021/ma302641d>.
- [83] P. Xiao, F. Dumur, M. Frigoli, B. Graff, F. Morlet-Savary, G. Wantz, H. Bock, J.P. Fouassier, D. Gigmes, J. Lalevée, Perylene derivatives as photoinitiators in blue light sensitive cationic or radical curable films and panchromatic thiol-ene polymerizable films, *European Polymer Journal* 53 (2014) 215–222. <https://doi.org/10.1016/j.eurpolymj.2014.01.024>.
- [84] J. Zhang, F. Dumur, M. Bouzrati, P. Xiao, C. Dietlin, F. Morlet-Savary, B. Graff, D. Gigmes, J.P. Fouassier, J. Lalevée, Novel panchromatic photopolymerizable matrices: N,N'-dibutylquinacridone as an efficient and versatile photoinitiator, *Journal of Polymer Science Part A: Polymer Chemistry* 53 (2015) 1719–1727. <https://doi.org/10.1002/pola.27615>.
- [85] P. Xiao, F. Dumur, T.T. Bui, F. Goubard, B. Graff, F. Morlet-Savary, J.P. Fouassier, D. Gigmes, J. Lalevée, Panchromatic Photopolymerizable Cationic Films Using Indoline and Squaraine Dye Based Photoinitiating Systems, *ACS Macro Lett.* 2 (2013) 736–740. <https://doi.org/10.1021/mz400316y>.
- [86] J. Zhang, N. Zivic, F. Dumur, C. Guo, Y. Li, P. Xiao, B. Graff, D. Gigmes, J.P. Fouassier, J. Lalevée, Panchromatic photoinitiators for radical, cationic and thiol-ene polymerization reactions: A search in the diketopyrrolopyrrole or indigo dye series, *Materials Today Communications* 4 (2015) 101–108. <https://doi.org/10.1016/j.mtcomm.2015.06.007>.
- [87] G.E. Cagnetta, A. Gallastegui, S.R. Martínez, D. Mantione, M. Criado-Gonzalez, M. Regato-Herbella, L. Lezama, R.E. Palacios, M.L. Gómez, D. Mecerreyes, C.A. Chesta, Conjugated Polymer Nanoparticles as Visible Light Panchromatic Photoinitiators for 3D Printing of Acrylic Hydrogels, *Macromolecules* 57 (2024) 78–87. <https://doi.org/10.1021/acs.macromol.3c02026>.
- [88] K. Starzak, W. Tomal, A. Chachaj-Brekiesz, M. Galek, J. Ortyl, Revealing the photoredox potential of azulene derivatives as panchromatic photoinitiators in various light-initiated polymerization processes, *Polym. Chem.* (2024). <https://doi.org/10.1039/D4PY00275J>.
- [89] S. Telitel, F. Dumur, M. Lepeltier, D. Gigmes, J.-P. Fouassier, J. Lalevée, Photoredox process induced polymerization reactions: Iridium complexes for panchromatic photoinitiating systems, *Comptes Rendus Chimie* 19 (2016) 71–78. <https://doi.org/10.1016/j.crci.2015.06.016>.
- [90] A. Balcerak, J. Kabatc-Borcz, Z. Czech, M. Bartkowiak, Latest Advances in Highly Efficient Dye-Based Photoinitiating Systems for Radical Polymerization, *Polymers* 15 (2023). <https://doi.org/10.3390/polym15051148>.

- [91] M.-A. Tehfe, F. Dumur, P. Xiao, B. Graff, F. Morlet-Savary, J.-P. Fouassier, D. Gignes, J. Lalevée, New chromone based photoinitiators for polymerization reactions under visible light, *Polym. Chem.* 4 (2013) 4234–4244. <https://doi.org/10.1039/C3PY00536D>.
- [92] J. You, H. Fu, D. Zhao, T. Hu, J. Nie, T. Wang, Flavonol dyes with different substituents in photopolymerization, *Journal of Photochemistry and Photobiology A: Chemistry* 386 (2020) 112097. <https://doi.org/10.1016/j.jphotochem.2019.112097>.
- [93] A. Al Mousawi, P. Garra, M. Schmitt, J. Toufaily, T. Hamieh, B. Graff, J.P. Fouassier, F. Dumur, J. Lalevée, 3-Hydroxyflavone and N-Phenylglycine in High Performance Photoinitiating Systems for 3D Printing and Photocomposites Synthesis, *Macromolecules* 51 (2018) 4633–4641. <https://doi.org/10.1021/acs.macromol.8b00979>.
- [94] E.A. Kamoun, A. Winkel, M. Eisenburger, H. Menzel, Carboxylated camphorquinone as visible-light photoinitiator for biomedical application: Synthesis, characterization, and application, *Arabian Journal of Chemistry* 9 (2016) 745–754. <https://doi.org/10.1016/j.arabjc.2014.03.008>.
- [95] A. Santini, I.T. Gallegos, C.M. Felix, Photoinitiators in Dentistry: A Review, *Prim Dent J* 2 (2013) 30–33. <https://doi.org/10.1308/205016814809859563>.
- [96] J. Zhao, J. Lalevée, H. Lu, R. MacQueen, S.H. Kable, T.W. Schmidt, M.H. Stenzel, P. Xiao, A new role of curcumin: as a multicolor photoinitiator for polymer fabrication under household UV to red LED bulbs, *Polym. Chem.* 6 (2015) 5053–5061. <https://doi.org/10.1039/C5PY00661A>.
- [97] J.V. Crivello, U. Bulut, Curcumin: A naturally occurring long-wavelength photosensitizer for diaryliodonium salts, *Journal of Polymer Science Part A: Polymer Chemistry* 43 (2005) 5217–5231. <https://doi.org/10.1002/pola.21017>.
- [98] W. Han, H. Fu, T. Xue, T. Liu, Y. Wang, T. Wang, Facilely prepared blue-green light sensitive curcuminoids with excellent bleaching properties as high performance photosensitizers in cationic and free radical photopolymerization, *Polym. Chem.* 9 (2018) 1787–1798. <https://doi.org/10.1039/C8PY00166A>.
- [99] A. Mishra, S. Daswal, Curcumin, A Novel Natural Photoinitiator for the Copolymerization of Styrene and Methylmethacrylate, *Null* 42 (2005) 1667–1678. <https://doi.org/10.1080/10601320500246974>.
- [100] L. Breloy, V. Brezová, S. Richeter, S. Clément, J.-P. Malval, S. Abbad Andaloussi, D.-L. Versace, Bio-based porphyrins pyropheophorbide a and its Zn-complex as visible-light photosensitizers for free-radical photopolymerization, *Polym. Chem.* 13 (2022) 1658–1671. <https://doi.org/10.1039/D1PY01714D>.
- [101] S. Shanmugam, J. Xu, C. Boyer, Utilizing the electron transfer mechanism of chlorophyll a under light for controlled radical polymerization, *Chem. Sci.* 6 (2015) 1341–1349. <https://doi.org/10.1039/C4SC03342F>.
- [102] L. Breloy, C. Negrell, A.-S. Mora, W.S.J. Li, V. Brezová, S. Caillol, D.-L. Versace, Vanillin derivative as performing type I photoinitiator, *European Polymer Journal* 132 (2020) 109727. <https://doi.org/10.1016/j.eurpolymj.2020.109727>.
- [103] H. Chen, D. Zhu, T. Kavalli, P. Xiao, M. Schmitt, J. Lalevée, Photopolymerization using bio-sourced photoinitiators, *Polym. Chem.* 14 (2023) 3543–3568. <https://doi.org/10.1039/D3PY00651D>.
- [104] T. Grune, G. Lietz, A. Palou, A.C. Ross, W. Stahl, G. Tang, D. Thurnham, S. Yin, H.K. Biesalski, β -Carotene Is an Important Vitamin A Source for Humans, *The Journal of Nutrition* 140 (2010) 2268S–2285S. <https://doi.org/10.3945/jn.109.119024>.

- [105] L. Breloy, C.A. Ouarabi, A. Brosseau, P. Dubot, V. Brezova, S. Abbad Andaloussi, J.-P. Malval, D.-L. Versace, β -Carotene/Limonene Derivatives/Eugenol: Green Synthesis of Antibacterial Coatings under Visible-Light Exposure, *ACS Sustainable Chem. Eng.* 7 (2019) 19591–19604. <https://doi.org/10.1021/acssuschemeng.9b04686>.
- [106] X. Xu, S. Awwad, L. Diaz-Gomez, C. Alvarez-Lorenzo, S. Brocchini, S. Gaisford, A. Goyanes, A.W. Basit, 3D Printed Punctal Plugs for Controlled Ocular Drug Delivery, *Pharmaceutics* 13 (2021). <https://doi.org/10.3390/pharmaceutics13091421>.
- [107] J. Field, J.W. Haycock, F.M. Boissonade, F. Claeysens, A Tuneable, Photocurable, Poly(Caprolactone)-Based Resin for Tissue Engineering—Synthesis, Characterisation and Use in Stereolithography, *Molecules* 26 (2021). <https://doi.org/10.3390/molecules26051199>.
- [108] S. Kim, C.-C. Chu, Visible light induced dextran-methacrylate hydrogel formation using (-)-riboflavin vitamin B2 as a photoinitiator and L-arginine as a co-initiator, *Fibers and Polymers* 10 (2009) 14–20. <https://doi.org/10.1007/s12221-009-0014-z>.
- [109] R. Huang, E. Choe, D.B. Min, Kinetics for Singlet Oxygen Formation by Riboflavin Photosensitization and the Reaction between Riboflavin and Singlet Oxygen, *Journal of Food Science* 69 (2004) C726–C732. <https://doi.org/10.1111/j.1365-2621.2004.tb09924.x>.
- [110] G.K. Oster, G. Oster, G. Prati, Dye-sensitized Photopolymerization of Acrylamide1, *J. Am. Chem. Soc.* 79 (1957) 595–598. <https://doi.org/10.1021/ja01560a025>.
- [111] P.G. Righetti, C. Gelfi, A.B. Bosisio, Polymerization kinetics of polyacrylamide gels. III. Effect of catalysts, *ELECTROPHORESIS* 2 (1981) 291–295. <https://doi.org/10.1002/elps.1150020507>.
- [112] M.V. Encinas, A.M. Rufs, S. Bertolotti, C.M. Previtali, Free Radical Polymerization Photoinitiated by Riboflavin/Amines. Effect of the Amine Structure, *Macromolecules* 34 (2001) 2845–2847. <https://doi.org/10.1021/ma001649r>.
- [113] E. Kim, M.H. Kim, J.H. Song, C. Kang, W.H. Park, Dual crosslinked alginate hydrogels by riboflavin as photoinitiator, *International Journal of Biological Macromolecules* 154 (2020) 989–998. <https://doi.org/10.1016/j.ijbiomac.2020.03.134>.
- [114] S.G. Bertolotti, C.M. Previtali, A.M. Rufs, M.V. Encinas, Riboflavin/Triethanolamine as Photoinitiator System of Vinyl Polymerization. A Mechanistic Study by Laser Flash Photolysis, *Macromolecules* 32 (1999) 2920–2924. <https://doi.org/10.1021/ma981246f>.
- [115] W.G. Santos, F. Mattiucci, S.J.L. Ribeiro, Polymerization Rate Modulated by Tetraarylborate Anion Structure: Direct Correlation of Hammett Substituent Constant with Polymerization Kinetics of 2-Hydroxyethyl Methacrylate, *Macromolecules* 51 (2018) 7905–7913. <https://doi.org/10.1021/acs.macromol.8b01361>.
- [116] W. Pan, T.J. Wallin, J. Odent, M.C. Yip, B. Mosadegh, R.F. Shepherd, E.P. Giannelis, Optical stereolithography of antifouling zwitterionic hydrogels, *J. Mater. Chem. B* 7 (2019) 2855–2864. <https://doi.org/10.1039/C9TB00278B>.
- [117] P. Demina, N. Arkharova, I. Asharchuk, K. Khaydukov, D. Karimov, V. Rocheva, A. Nechaev, Y. Grigoriev, A. Generalova, E. Khaydukov, Polymerization Assisted by Upconversion Nanoparticles under NIR Light, *Molecules* 24 (2019). <https://doi.org/10.3390/molecules24132476>.
- [118] T. Zhang, J. Yeow, C. Boyer, A cocktail of vitamins for aqueous RAFT polymerization in an open-to-air microtiter plate, *Polym. Chem.* 10 (2019) 4643–4654. <https://doi.org/10.1039/C9PY00898E>.

- [119] I. Zaborniak, P. Chmielarz, K. Matyjaszewski, Modification of wood-based materials by atom transfer radical polymerization methods, *European Polymer Journal* 120 (2019) 109253. <https://doi.org/10.1016/j.eurpolymj.2019.109253>.
- [120] I. Zaborniak, P. Chmielarz, K. Matyjaszewski, Synthesis of Riboflavin-Based Macromolecules through Low ppm ATRP in Aqueous Media, *Macromolecular Chemistry and Physics* 221 (2020) 1900496. <https://doi.org/10.1002/macp.201900496>.
- [121] I. Zaborniak, K. Surmacz, M. Flejszar, P. Chmielarz, Triple-functional riboflavin-based molecule for efficient atom transfer radical polymerization in miniemulsion media, *Journal of Applied Polymer Science* 137 (2020) 49275. <https://doi.org/10.1002/app.49275>.
- [122] P. Sautrot-Ba, J.-P. Malval, M. Weiss-Maurin, J. Paul, A. Blacha-Grzechnik, S. Tomane, P.-E. Mazeran, J. Lalevée, V. Langlois, D.-L. Versace, Paprika, Gallic Acid, and Visible Light: The Green Combination for the Synthesis of Biocide Coatings, *ACS Sustainable Chem. Eng.* 6 (2018) 104–109. <https://doi.org/10.1021/acssuschemeng.7b03723>.
- [123] T. Borjigin, J. Feng, M. Schmitt, D. Zhu, F. Morlet-Savary, P. Xiao, J. Lalevée, Photoinitiators from bio-sourced naphthoquinone – the application of naphthoquinone-based vitamins K1 and K3 in free radical photopolymerization, *Green Chem.* 26 (2024) 277–286. <https://doi.org/10.1039/D3GC03551D>.
- [124] T. Urano, H. Ito, K. Takahama, T. Yamaoka, Photopolymerization mechanisms of acrylates in poly(methyl methacrylate) films, *Polymers for Advanced Technologies* 10 (1999) 201–205. [https://doi.org/10.1002/\(SICI\)1099-1581\(199904\)10:4<201::AID-PAT860>3.0.CO;2-U](https://doi.org/10.1002/(SICI)1099-1581(199904)10:4<201::AID-PAT860>3.0.CO;2-U).
- [125] C. Elian, V. Brezová, P. Sautrot-Ba, M. Breza, D.-L. Versace, Lawsone Derivatives as Efficient Photopolymerizable Initiators for Free-Radical, Cationic Photopolymerizations, and Thiol–Ene Reactions, *Polymers* 13 (2021). <https://doi.org/10.3390/polym13122015>.
- [126] R. Strzelczyk, R. Podsiadły, Derivatives of 1,4-naphthoquinone as visible-light-absorbing one-component photoinitiators for radical polymerisation, *Coloration Technology* 131 (2015) 229–235. <https://doi.org/10.1111/cote.12144>.
- [127] A.M. Szymczak, R. Podsiadły, K. Podemska, J. Sokołowska, Dyes based on a 1,4-naphthoquinone skeleton as new type II photoinitiators for radical polymerisation, *Coloration Technology* 129 (2013) 284–288. <https://doi.org/10.1111/cote.12030>.
- [128] X. Peng, D. Zhu, P. Xiao, Naphthoquinone derivatives: Naturally derived molecules as blue-light-sensitive photoinitiators of photopolymerization, *European Polymer Journal* 127 (2020) 109569. <https://doi.org/10.1016/j.eurpolymj.2020.109569>.
- [129] Tikhomirov S. Alexander, Shtil A. Alexander, Shchekotikhin E. Andrey, Advances in the Discovery of Anthraquinone-Based Anticancer Agents, *Recent Patents on Anti-Cancer Drug Discovery* 13 (2018) 159–183. <https://doi.org/10.2174/1574892813666171206123114>.
- [130] W. Tian, C. Wang, D. Li, H. Hou, Novel Anthraquinone Compounds as Anticancer Agents and their Potential Mechanism, *Future Medicinal Chemistry* 12 (2020) 627–644. <https://doi.org/10.4155/fmc-2019-0322>.
- [131] X. Peng, J. Zhang, M.M. Banaszak Holl, P. Xiao, Thiol-Ene Photopolymerization under Blue, Green and Red LED Irradiation, *ChemPhotoChem* 5 (2021) 571–581. <https://doi.org/10.1002/cptc.202100028>.
- [132] V.K. Tandon, M.K. Verma, H.K. Maurya, S. Kumar, Micelles catalyzed one pot regio- and chemoselective synthesis of benzo[a]phenazines and naphtho[2,3-d]imidazoles ‘in H₂O,’ *Tetrahedron Letters* 55 (2014) 6331–6334. <https://doi.org/10.1016/j.tetlet.2014.09.103>.

- [133] A.A. Aly, A.A. Hassan, A.B. Brown, K.M. El-Shaieb, T.M.I. Bedair, Facile synthesis of new imidazoles from direct reaction of 2,3-diamino-1,4-naphthoquinone with aldehydes, *Journal of Heterocyclic Chemistry* 48 (2011) 787–791. <https://doi.org/10.1002/jhet.582>.
- [134] L. Tan, H. Shan, C. Han, Z. Zhang, J. Shen, X. Zhang, H. Xiang, K. Lu, C. Qi, Y. Li, G. Zhuang, G. Chen, L. Tan, Discovery of Potent OTUB1/USP8 Dual Inhibitors Targeting Proteostasis in Non-Small-Cell Lung Cancer, *J. Med. Chem.* 65 (2022) 13645–13659. <https://doi.org/10.1021/acs.jmedchem.2c00408>.
- [135] Z. Liu, Z. Zhang, W. Zhang, D. Yan, 2-Substituted-1-(2-morpholinoethyl)-1H-naphtho[2,3-d]imidazole-4,9-diones: Design, synthesis and antiproliferative activity, *Bioorganic & Medicinal Chemistry Letters* 28 (2018) 2454–2458. <https://doi.org/10.1016/j.bmcl.2018.06.007>.
- [136] L.M. Gornostaev, M.V. Vigant, O.I. Kargina, A.S. Kuznetsova, Yu.G. Khalyavina, T.I. Lavrikova, Synthesis of 2-aryl-1-hydroxy-1H-naphtho[2,3-d]imidazole-4,9-diones by reaction of 2-benzylamino-1,4-naphthoquinones with nitric acid, *Russian Journal of Organic Chemistry* 49 (2013) 1354–1357. <https://doi.org/10.1134/S1070428013090194>.
- [137] Z. Yu, J. Su, C. Huang, J. Wei, L. Han, Q. Ye, Y. Li, Base-promoted Oxidative Sulfuration/Cyclization to Construct Naphtho[2,3-d]thiazole through Three-component Reaction Using S8 as the Sulfur Source, *Asian Journal of Organic Chemistry* 11 (2022) e202200288. <https://doi.org/10.1002/ajoc.202200288>.
- [138] O. Lavergne, A.-C. Fernandes, L. Bréhu, A. Sidhu, M.-C. Brézak, G. Prévost, B. Ducommun, M.-O. Contour-Galcera, Synthesis and biological evaluation of novel heterocyclic quinones as inhibitors of the dual specificity protein phosphatase CDC25C, *Bioorganic & Medicinal Chemistry Letters* 16 (2006) 171–175. <https://doi.org/10.1016/j.bmcl.2005.09.030>.
- [139] S. Liu, D. Brunel, K. Sun, Y. Xu, F. Morlet-Savary, B. Graff, P. Xiao, F. Dumur, J. Lalevée, A monocomponent bifunctional benzophenone–carbazole type II photoinitiator for LED photoinitiating systems, *Polym. Chem.* 11 (2020) 3551–3556. <https://doi.org/10.1039/D0PY00644K>.
- [140] S. Liu, H. Chen, Y. Zhang, K. Sun, Y. Xu, F. Morlet-Savary, B. Graff, G. Noirbent, C. Pigot, D. Brunel, M. Nechab, D. Gignes, P. Xiao, F. Dumur, J. Lalevée, Monocomponent Photoinitiators based on Benzophenone–Carbazole Structure for LED Photoinitiating Systems and Application on 3D Printing, *Polymers* 12 (2020) 1394. <https://doi.org/10.3390/polym12061394>.
- [141] F. Dumur, Recent Advances in Monocomponent Visible Light Photoinitiating Systems Based on Sulfonium Salts, *Polymers* 15 (2023). <https://doi.org/10.3390/polym15214202>.
- [142] F. Dumur, Recent Advances on Diaryliodonium-Based Monocomponent Photoinitiating Systems, *European Polymer Journal* (2023) 112193. <https://doi.org/10.1016/j.eurpolymj.2023.112193>.
- [143] M. Topa-Skwarczyńska, F. Petko, D. Krok, M. Galek, J. Ortyl, High-performance new photoinitiators for the preparation of functional photocurable polymer composites, *European Polymer Journal* 196 (2023) 112282. <https://doi.org/10.1016/j.eurpolymj.2023.112282>.
- [144] F. Petko, M. Galek, E. Hola, M. Topa-Skwarczyńska, W. Tomal, M. Jankowska, M. Pilch, R. Popielarz, B. Graff, F. Morlet-Savary, J. Lalevee, J. Ortyl, Symmetric Iodonium Salts Based on Benzylidene as One-Component Photoinitiators for Applications in 3D

- Printing, *Chem. Mater.* 34 (2022) 10077–10092.
<https://doi.org/10.1021/acs.chemmater.2c02796>.
- [145] J.-P. Fouassier, J. Lalevée, *Photoinitiators: Structures, Reactivity and Applications in Polymerization*, Wiley-VCH, 2021.
- [146] J.-Y. Yao, H.-H. Hou, X.-D. Ma, H.-J. Xu, Z.-X. Shi, J. Yin, X.-S. Jiang, Combining photo-cleavable and hydrogen-abstracting groups in quinoxaline with thioether bond as hybrid photoinitiator, *Chinese Chemical Letters* 28 (2017) 6–12.
<https://doi.org/10.1016/j.ccl.2016.06.008>.
- [147] S. Liu, T. Borjigin, M. Schmitt, F. Morlet-Savary, P. Xiao, J. Lalevée, High-Performance Photoinitiating Systems for LED-Induced Photopolymerization, *Polymers* 15 (2023).
<https://doi.org/10.3390/polym15020342>.
- [148] M.-A. Tehfe, F. Dumur, B. Graff, F. Morlet-Savary, D. Gigmes, J.-P. Fouassier, J. Lalevée, Design of new Type I and Type II photoinitiators possessing highly coupled pyrene–ketone moieties, *Polym. Chem.* 4 (2013) 2313–2324.
<https://doi.org/10.1039/C3PY21079K>.
- [149] J. Xu, G. Ma, K. Wang, J. Gu, S. Jiang, J. Nie, Synthesis and photopolymerization kinetics of oxime ester photoinitiators, *Journal of Applied Polymer Science* 123 (2012) 725–731. <https://doi.org/10.1002/app.34551>.
- [150] K. Dietliker, T. Jung, J. Benkhoff, H. Kura, A. Matsumoto, H. Oka, D. Hristova, G. Gescheidt, G. Rist, New Developments in Photoinitiators, *Macromolecular Symposia* 217 (2004) 77–98. <https://doi.org/10.1002/masy.200451307>.
- [151] A. Kowalska, J. Sokolowski, K. Bociog, The Photoinitiators Used in Resin Based Dental Composite—A Review and Future Perspectives, *Polymers* 13 (2021).
<https://doi.org/10.3390/polym13030470>.
- [152] C. Dietlin, T.T. Trinh, S. Schweizer, B. Graff, F. Morlet-Savary, P.-A. Noirot, J. Lalevée, New Phosphine Oxides as High Performance Near-UV Type I Photoinitiators of Radical Polymerization, *Molecules* 25 (2020). <https://doi.org/10.3390/molecules25071671>.
- [153] M.A. Lago, A.R.-B. de Quirós, R. Sendón, J. Bustos, M.T. Nieto, P. Paseiro, Photoinitiators: a food safety review, *Food Additives & Contaminants: Part A* 32 (2015) 779–798. <https://doi.org/10.1080/19440049.2015.1014866>.
- [154] F. Hammoud, A. Pavlou, A. Petropoulos, B. Graff, M.G. Siskos, A. Hijazi, F. Morlet-Savary, F. Dumur, J. Lalevée, Naphthoquinone-based imidazolyl esters as blue-light-sensitive Type I photoinitiators, *Polym. Chem.* 13 (2022) 4817–4831.
<https://doi.org/10.1039/D2PY00753C>.
- [155] S. Chen, M. Jin, J.-P. Malval, J. Fu, F. Morlet-Savary, H. Pan, D. Wan, Substituted stilbene-based oxime esters used as highly reactive wavelength-dependent photoinitiators for LED photopolymerization, *Polym. Chem.* 10 (2019) 6609–6621.
<https://doi.org/10.1039/C9PY01330J>.
- [156] C. Elian, N. Sanosa, N. Bogliotti, C. Herrero, D. Sampedro, D.-L. Versace, An anthraquinone-based oxime ester as a visible-light photoinitiator for 3D photoprinting applications, *Polym. Chem.* 14 (2023) 3262–3269. <https://doi.org/10.1039/D3PY00681F>.
- [157] S. Fan, X. Sun, X. He, Y. Pang, Y. Xin, Y. Ding, Y. Zou, Coumarin Ketoxime Ester with Electron-Donating Substituents as Photoinitiators and Photosensitizers for Photopolymerization upon UV-Vis LED Irradiation, *Polymers* 14 (2022).
<https://doi.org/10.3390/polym14214588>.

- [158] D.E. Fast, A. Lauer, J.P. Menzel, A.-M. Kelterer, G. Gescheidt, C. Barner-Kowollik, Wavelength-Dependent Photochemistry of Oxime Ester Photoinitiators, *Macromolecules* 50 (2017) 1815–1823. <https://doi.org/10.1021/acs.macromol.7b00089>.
- [159] P. Hu, W. Qiu, S. Naumov, T. Scherzer, Z. Hu, Q. Chen, W. Knolle, Z. Li, Conjugated Bifunctional Carbazole-Based Oxime Esters: Efficient and Versatile Photoinitiators for 3D Printing under One- and Two-Photon Excitation, *ChemPhotoChem* 4 (2020) 224–232. <https://doi.org/10.1002/cptc.201900246>.
- [160] Z. Li, X. Zou, G. Zhu, X. Liu, R. Liu, Coumarin-Based Oxime Esters: Photobleachable and Versatile Unimolecular Initiators for Acrylate and Thiol-Based Click Photopolymerization under Visible Light-Emitting Diode Light Irradiation, *ACS Appl. Mater. Interfaces* 10 (2018) 16113–16123. <https://doi.org/10.1021/acsami.8b01767>.
- [161] Z.-H. Lee, S.-C. Yen, F. Hammoud, A. Hijazi, B. Graff, J. Lalevée, Y.-C. Chen, Naphthalene-Based Oxime Esters as Type I Photoinitiators for Free Radical Photopolymerization, *Polymers* 14 (2022). <https://doi.org/10.3390/polym14235261>.
- [162] X. Ma, D. Cao, H. Fu, J. You, R. Gu, B. Fan, J. Nie, T. Wang, Multicomponent photoinitiating systems containing arylamino oxime ester for visible light photopolymerization, *Progress in Organic Coatings* 135 (2019) 517–524. <https://doi.org/10.1016/j.porgcoat.2019.06.027>.
- [163] H. Lu, Z. Li, Synthesis and Structure-Activity Relationship of N-Substituted Carbazole Oxime Ester Photoinitiators, *Journal of Photopolymer Science and Technology* 34 (2021) 307–313. <https://doi.org/10.2494/photopolymer.34.307>.
- [164] Y. Pang, S. Fan, Q. Wang, D. Oprych, A. Feilen, K. Reiner, D. Keil, Y.L. Slominsky, S. Popov, Y. Zou, B. Strehmel, NIR-Sensitized Activated Photoreaction between Cyanines and Oxime Esters: Free-Radical Photopolymerization, *Angewandte Chemie International Edition* 59 (2020) 11440–11447. <https://doi.org/10.1002/anie.202004413>.
- [165] W. Qiu, J. Zhu, K. Dietliker, Z. Li, Polymerizable Oxime Esters: An Efficient Photoinitiator with Low Migration Ability for 3D Printing to Fabricate Luminescent Devices, *ChemPhotoChem* 4 (2020) 5296–5303. <https://doi.org/10.1002/cptc.202000146>.
- [166] Y. Muramatsu, M. Kaji, A. Unno, O. Hirai, Terminal Group Analyses of Photopolymerized Products Using a MALDI-TOFMS for the Study on the Oxime Ester type Photoinitiators, *Journal of Photopolymer Science and Technology* 23 (2010) 447–450. <https://doi.org/10.2494/photopolymer.23.447>.
- [167] J. Akhigbe, M. Luciano, M. Zeller, C. Brückner, Mono- and Bisquinoline-Annulated Porphyrins from Porphyrin β, β' -Dione Oximes, *J. Org. Chem.* 80 (2015) 499–511. <https://doi.org/10.1021/jo502511j>.
- [168] J. Duan, Y. Cheng, R. Li, P. Li, Synthesis of spiro[indane-1,3-dione-1-pyrrolines] via copper-catalyzed heteroannulation of ketoxime acetates with 2-arylideneindane-1,3-diones, *Org. Chem. Front.* 3 (2016) 1614–1618. <https://doi.org/10.1039/C6QO00454G>.
- [169] A. Barve, M. Noolvi, N. Subhedar, V.D. Gupta, G. Bhatia, Synthesis and antimicrobial activity of novel oxime derivatives of phenothiazine, *European Journal of Chemistry* 2 (2011) 388–393. <https://doi.org/10.5155/eurjchem.2.3.388-393.184>.
- [170] AllonasXavier, LalevéeJacques, FouassierJean-Pierre, TachiHideki, ShiraiMasamitsu, TsunookaMasahiro, Triplet State of O-Acyloximes Studied by Time-Resolved Absorption Spectroscopy, *Chemistry Letters* 29 (2004) 1090–1091. <https://doi.org/10.1246/cl.2000.1090>.
- [171] J. Lalevée, X. Allonas, J.P. Fouassier, H. Tachi, A. Izumitani, M. Shirai, M. Tsunooka, Investigation of the photochemical properties of an important class of photobase

- generators: the O-acyloximes, *Journal of Photochemistry and Photobiology A: Chemistry* 151 (2002) 27–37. [https://doi.org/10.1016/S1010-6030\(02\)00174-0](https://doi.org/10.1016/S1010-6030(02)00174-0).
- [172] R.K. Jha, M. Batabyal, S. Kumar, Blue Light Irradiated Metal-, Oxidant-, and Base-Free Cross-Dehydrogenative Coupling of C(sp²)-H and N-H Bonds: Amination of Naphthoquinones with Amines, *J. Org. Chem.* 88 (2023) 7401–7424. <https://doi.org/10.1021/acs.joc.3c00666>.
- [173] X. Wu, X.-J. Zhao, L. Zhang, G. Li, Y. He, Electrooxidative dehydrogenative coupling of 1,4-naphthoquinones with amines: Facile access to 2-amino-1,4-naphthoquinones, *Tetrahedron Letters* 112 (2022) 154208. <https://doi.org/10.1016/j.tetlet.2022.154208>.
- [174] C.Y. Bon, S. Mugohera, K.S. Lee, J.H. Park, H. Kwon, J. Park, J.M. Ko, S.-I. Yoo, 2-anilino-1,4-naphthoquinone and 2-benzylamino-1,4-naphthoquinone with activated carbon composite electrodes for supercapacitor application, *Colloids and Surfaces A: Physicochemical and Engineering Aspects* 687 (2024) 133445. <https://doi.org/10.1016/j.colsurfa.2024.133445>.
- [175] V.K. Singh, S.K. Verma, R. Kadu, S.M. Mobin, Identification of unusual C-Cl \cdots π contacts in 2-(alkylamino)-3-chloro-1,4-naphthoquinones: effect of N-substituents on crystal packing, fluorescence, redox and anti-microbial properties, *RSC Adv.* 5 (2015) 43669–43686. <https://doi.org/10.1039/C5RA02295A>.
- [176] B.C. Lemos, R. Westphal, E.V. Filho, R.G. Fiorot, J.W.M. Carneiro, A.C.C. Gomes, C.J. Guimarães, F.C.E. de Oliveira, P.M.S. Costa, C. Pessoa, S.J. Greco, Synthetic enamine naphthoquinone derived from lawsone as cytotoxic agents assessed by in vitro and in silico evaluations, *Bioorganic & Medicinal Chemistry Letters* 53 (2021) 128419. <https://doi.org/10.1016/j.bmcl.2021.128419>.
- [177] B.J. Josey, E.S. Inks, X. Wen, C.J. Chou, Structure-Activity Relationship Study of Vitamin K Derivatives Yields Highly Potent Neuroprotective Agents, *J. Med. Chem.* 56 (2013) 1007–1022. <https://doi.org/10.1021/jm301485d>.
- [178] E.S. Inks, B.J. Josey, S.R. Jesinkey, C.J. Chou, A Novel Class of Small Molecule Inhibitors of HDAC6, *ACS Chem. Biol.* 7 (2012) 331–339. <https://doi.org/10.1021/cb200134p>.
- [179] Q. Zhang, C.-W.T. Chang, Divergent and facile Lewis acid-mediated synthesis of N-alkyl 2-aminomethylene-1,3-indanediones and 2-alkylamino-1,4-naphthoquinones, *Tetrahedron Letters* 56 (2015) 893–896. <https://doi.org/10.1016/j.tetlet.2015.01.014>.
- [180] L.S. Konstantinova, K.A. Lysov, L.I. Souvorova, O.A. Rakitin, Synthesis of 2,3-dihydronaphtho[2,3-d][1,3]thiazole-4,9-diones and 2,3-dihydroanthra[2,3-d][1,3]thiazole-4,11-diones and novel ring contraction and fusion reaction of 3H-spiro[1,3-thiazole-2,1'-cyclohexanes] into 2,3,4,5-tetrahydro-1H-carbazole-6,11-diones, *Beilstein J. Org. Chem.* 9 (2013) 577–584. <https://doi.org/10.3762/bjoc.9.62>.
- [181] S. Sar, J. Chauhan, S. Sen, Generation of Aryl Radicals from Aryl Hydrazines via Catalytic Iodine in Air: Arylation of Substituted 1,4-Naphthoquinones, *ACS Omega* 5 (2020) 4213–4222. <https://doi.org/10.1021/acsomega.9b04014>.
- [182] J.C. Warner, A.S. Cannon, K.M. Dye, Green chemistry, *Environmental Impact Assessment Review* 24 (2004) 775–799. <https://doi.org/10.1016/j.eiar.2004.06.006>.
- [183] R.A. Sheldon, The E factor at 30: a passion for pollution prevention, *Green Chem.* 25 (2023) 1704–1728. <https://doi.org/10.1039/D2GC04747K>.
- [184] R.A. Sheldon, The E factor 25 years on: the rise of green chemistry and sustainability, *Green Chem.* 19 (2017) 18–43. <https://doi.org/10.1039/C6GC02157C>.

- [185] F. Hammoud, N. Giacoletto, G. Noirbent, B. Graff, A. Hijazi, M. Nechab, D. Gignes, F. Dumur, J. Lalevée, Substituent effects on the photoinitiation ability of coumarin-based oxime-ester photoinitiators for free radical photopolymerization, *Mater. Chem. Front.* 5 (2021) 8361–8370. <https://doi.org/10.1039/D1QM01310F>.
- [186] F. Hammoud, N. Giacoletto, M. Nechab, B. Graff, A. Hijazi, F. Dumur, J. Lalevée, 5,12-Dialkyl-5,12-dihydroindolo[3,2-a]carbazole-Based Oxime-Esters for LED Photoinitiating Systems and Application on 3D Printing, *Macromolecular Materials and Engineering* 307 (2022) 2200082. <https://doi.org/10.1002/mame.202200082>.
- [187] M. Rahal, H. Bidotti, S. Duval, B. Graff, T. Hamieh, J. Toufaily, F. Dumur, J. Lalevée, Investigation of pyrene vs Anthracene-based oxime esters: Role of the excited states on their polymerization initiating abilities, *European Polymer Journal* 177 (2022) 111452. <https://doi.org/10.1016/j.eurpolymj.2022.111452>.
- [188] F. Hammoud, A. Hijazi, M. Schmitt, F. Dumur, J. Lalevée, A review on recently proposed oxime ester photoinitiators, *European Polymer Journal* 188 (2023) 111901. <https://doi.org/10.1016/j.eurpolymj.2023.111901>.
- [189] J.-B. Hsieh, S.-C. Yen, F. Hammoud, J. Lalevée, Y.-C. Chen, Effect of Terminal Alkyl Chains for Free Radical Photopolymerization Based on Triphenylamine Oxime Ester Visible-Light Absorbing Type I Photoinitiators, *ChemistrySelect* 8 (2023) e202301297. <https://doi.org/10.1002/slct.202301297>.
- [190] Y. Wang, R. Chen, D. Liu, C. Peng, J. Wang, X. Dong, New functionalized thioxanthone derivatives as type I photoinitiators for polymerization under UV-Vis LEDs, *New J. Chem.* 47 (2023) 5330–5337. <https://doi.org/10.1039/D2NJ05996G>.
- [191] T. Borjigin, M. Schmitt, N. Giacoletto, A. Rico, H. Bidotti, M. Nechab, Y. Zhang, B. Graff, F. Morlet-Savary, P. Xiao, F. Dumur, J. Lalevée, The Blue-LED-Sensitive Naphthoquinone-Imidazolyl Derivatives as Type II Photoinitiators of Free Radical Photopolymerization, *Advanced Materials Interfaces* 10 (2023) 2202352. <https://doi.org/10.1002/admi.202202352>.
- [192] Anzenbacher Pavel, M.A. Palacios, K. Jursíková, M. Marquez, Simple Electrooptical Sensors for Inorganic Anions, *Org. Lett.* 7 (2005) 5027–5030. <https://doi.org/10.1021/ol051992m>.
- [193] Z. Chen, J. Wang, T. Cai, Z. Hu, J. Chu, F. Wang, X. Gan, Z. Song, Constructing Extended π -Conjugated Molecules with o-Quinone Groups as High-Energy Organic Cathode Materials, *ACS Appl. Mater. Interfaces* 14 (2022) 27994–28003. <https://doi.org/10.1021/acsami.2c06252>.
- [194] N.N. Atia, P.Y. Khashaba, S.A. El Zohny, A.H. Rageh, Development of an innovative turn-on fluorescent probe for targeted in-vivo detection of nitric oxide in rat brain extracts as a biomarker for migraine disease, *Talanta* 272 (2024) 125763. <https://doi.org/10.1016/j.talanta.2024.125763>.
- [195] Y. Zhu, W. Jin, H. Gao, Y. Chen, T.-R. Wu, D.-Y. Wu, Y. Huang, D. Guo, Z. Chen, Q. Huang, J. Cao, J. Xu, C3-symmetric trimeric imidazole naphthoquinone derivative with dual redox-active sites for high-performance cathodic lithium storage, *Chemical Engineering Journal* 462 (2023) 142229. <https://doi.org/10.1016/j.cej.2023.142229>.
- [196] H. Zhang, Q. Huang, X. Xia, Y. Shi, Y.-M. Shen, J. Xu, Z. Chen, J. Cao, Aqueous organic redox-targeting flow battery based on Nernstian-potential-driven anodic redox-targeting reactions, *J. Mater. Chem. A* 10 (2022) 6740–6747. <https://doi.org/10.1039/D1TA10763A>.

- [197] J. Lee, H. Kim, M.J. Park, Long-Life, High-Rate Lithium-Organic Batteries Based on Naphthoquinone Derivatives, *Chem. Mater.* 28 (2016) 2408–2416. <https://doi.org/10.1021/acs.chemmater.6b00624>.
- [198] R. Manivannan, A. Satheshkumar, E.-S.H. El-Mossalamy, L.M. Al-Harbi, S.A. Kosa, K.P. Elango, Design, synthesis and characterization of indole based anion sensing receptors, *New J. Chem.* 39 (2015) 3936–3947. <https://doi.org/10.1039/C4NJ01728E>.
- [199] P.R. Lakshmi, P. Jayasudha, K.P. Elango, Selective chromogenic detection of cyanide in aqueous solution – Spectral, electrochemical and theoretical studies, *Spectrochimica Acta Part A: Molecular and Biomolecular Spectroscopy* 213 (2019) 318–323. <https://doi.org/10.1016/j.saa.2019.01.074>.
- [200] V. Remusat, T. Terme, A. Gellis, P. Rathelot, P. Vanelle, Synthesis of original benzo[g]quinoxaline-5,10-diones by bis-SRN1 methodology, *Journal of Heterocyclic Chemistry* 41 (2004) 221–225. <https://doi.org/10.1002/jhet.5570410212>.
- [201] I. Antonini, F. Claudi, G. Cristalli, M. Grifantini, S. Martelli, Acid-catalysed, nucleophile-catalysed and thermal decomposition of 2-amino-3-(2',2'-dimethylaziridino)-1,4-naphthoquinone, *Journal of Heterocyclic Chemistry* 17 (1980) 181–185. <https://doi.org/10.1002/jhet.5570170135>.
- [202] Y. Shao, X. He, Y. Xin, Y. Zhang, D. Zhang, L. Duan, Y. Zou, New Application of Multiresonance Organic Delayed Fluorescence Dyes: High-Performance Photoinitiating Systems for Acrylate and Epoxy Photopolymerization and Photoluminescent Pattern Preparation, *ACS Appl. Mater. Interfaces* 16 (2024) 30344–30354. <https://doi.org/10.1021/acsami.4c02834>.
- [203] M. Le Dot, E. Sprick, M.-L. Werth, G. Schrodj, B. Graff, D. Zeigler, C. Bowden, C. Smith, J. Jouanneau, P. Gérard, J. Lalevée, New bio-sourced monomer based on sesamol for copolymerization with Elium® resins and its depolymerization behavior, *European Polymer Journal* 213 (2024) 113091. <https://doi.org/10.1016/j.eurpolymj.2024.113091>.
- [204] X. Zhao, B. Hu, Q. Zhou, Y. Yu, E. Hao, X. Guo, Y. Xu, C. Yu, K. Sun, J. Lalevée, Triphenylamine-substituted BODIPY dye based photoinitiators for free radical and cationic photopolymerization under visible LED irradiation and application in 3D printing, *Dyes and Pigments* 222 (2024) 111880. <https://doi.org/10.1016/j.dyepig.2023.111880>.
- [205] E. Hola, F. Morlet-Savary, J. Lalevée, J. Ortyl, Photoinitiator or photosensitizer? Dual behaviour of m-terphenyls in photopolymerization processes, *European Polymer Journal* 189 (2023) 111971. <https://doi.org/10.1016/j.eurpolymj.2023.111971>.
- [206] L.M. Alhomaidan, H. Tar, A.S. Alnafisah, L.M. Aroua, N. Kouki, F.M. Alminderej, J. Lalevee, Copper II Complexes Based on Benzimidazole Ligands as a Novel Photoredox Catalysis for Free Radical Polymerization Embedded Gold and Silver Nanoparticles, *Polymers* 15 (2023). <https://doi.org/10.3390/polym15051289>.
- [207] E. Sprick, J.-M. Becht, T. Tigges, K. Neuhaus, C. Weber, J. Lalevée, Design of New Amines of Low Toxicity for Efficient Free Radical Polymerization under Air, *Macromolecular Chemistry and Physics* 221 (2020) 2000211. <https://doi.org/10.1002/macp.202000211>.
- [208] M.A. Tasdelen, J. Lalevée, Y. Yagci, Photoinduced free radical promoted cationic polymerization 40 years after its discovery, *Polym. Chem.* 11 (2020) 1111–1121. <https://doi.org/10.1039/C9PY01903K>.

- [209] T.N. Eren, B. Graff, J. Lalevée, D. Avci, Thioxanthone-functionalized 1,6-heptadiene as monomeric photoinitiator, *Progress in Organic Coatings* 128 (2019) 148–156. <https://doi.org/10.1016/j.porgcoat.2018.12.014>.
- [210] J. Zhang, J. Lalevée, F. Morlet-Savary, B. Graff, P. Xiao, Photopolymerization under various monochromatic UV/visible LEDs and IR lamp: Diamino-anthraquinone derivatives as versatile multicolor photoinitiators, *European Polymer Journal* 112 (2019) 591–600. <https://doi.org/10.1016/j.eurpolymj.2018.10.021>.
- [211] J.C. Walton, Functionalised Oximes: Emergent Precursors for Carbon-, Nitrogen- and Oxygen-Centred Radicals, *Molecules* 21 (2016). <https://doi.org/10.3390/molecules21010063>.
- [212] M. Devi, P. Kumar, R. Singh, J. Sindhu, R. Kataria, Design, synthesis, spectroscopic characterization, single crystal X-ray analysis, in vitro α -amylase inhibition assay, DPPH free radical evaluation and computational studies of naphtho[2,3-d]imidazole-4,9-dione appended 1,2,3-triazoles, *European Journal of Medicinal Chemistry* 250 (2023) 115230. <https://doi.org/10.1016/j.ejmech.2023.115230>.
- [213] J. Yuan, Z. Liu, Y. Dong, F. Gao, X. Xia, P. Wang, Y. Luo, Z. Zhang, D. Yan, W. Zhang, Pioneering 4,11-Dioxo-4,11-dihydro-1H-anthra[2,3-d]imidazol-3-ium Compounds as Promising Survivin Inhibitors by Targeting ILF3/NF110 for Cancer Therapy, *J. Med. Chem.* 66 (2023) 16843–16868. <https://doi.org/10.1021/acs.jmedchem.3c01551>.
- [214] Y. Zhang, B. Song, C. Dietlin, F. Morlet-Savary, M. Schmitt, F. Dumur, J. Lalevée, Naphthoquinone-Based Oxime Esters for Free Radical Photopolymerization under Sunlight or a Blue Light-Emitting Diode, *Ind. Eng. Chem. Res.* 63 (2024) 3962–3974. <https://doi.org/10.1021/acs.iecr.3c04378>.
- [215] N. Bao, J. Ou, W. Shi, N. Li, L. Chen, J. Sun, Highly Efficient Synthesis and Structure–Activity Relationships of a Small Library of Substituted 1,4-Naphthoquinones, *European Journal of Organic Chemistry* 2018 (2018) 2254–2258. <https://doi.org/10.1002/ejoc.201800207>.
- [216] Lachman, A., Noller, C.R., Benzophenone oxime, *Org. Synth.* 10 (1930) 10. <https://doi.org/10.15227/orgsyn.010.0010>.
- [217] W.-W. Fang, G.-Y. Yang, Z.-H. Fan, Z.-C. Chen, X.-L. Hu, Z. Zhan, I. Hussain, Y. Lu, T. He, B.-E. Tan, Conjugated cross-linked phosphine as broadband light or sunlight-driven photocatalyst for large-scale atom transfer radical polymerization, *Nature Communications* 14 (2023) 2891. <https://doi.org/10.1038/s41467-023-38402-y>.
- [218] M.L. Allegranza, Z.M. DeMartini, A.J. Kloster, Z.A. Digby, D. Konkolewicz, Visible and sunlight driven RAFT photopolymerization accelerated by amines: kinetics and mechanism, *Polym. Chem.* 7 (2016) 6626–6636. <https://doi.org/10.1039/C6PY01433J>.
- [219] C. Decker, T. Bendaikha, Interpenetrating polymer networks. II. Sunlight-induced polymerization of multifunctional acrylates, *Journal of Applied Polymer Science* 70 (1998) 2269–2282. [https://doi.org/10.1002/\(SICI\)1097-4628\(19981212\)70:11<2269::AID-APP21>3.0.CO;2-D](https://doi.org/10.1002/(SICI)1097-4628(19981212)70:11<2269::AID-APP21>3.0.CO;2-D).
- [220] J. Li, Q. Ding, K. Cao, Y. Chen, Z. Fu, J. Nie, Pyrrolidone based one-component photoinitiator for improving the storage stability of photocurable materials to sunlight via two beams of light excitation, *European Polymer Journal* 196 (2023) 112291. <https://doi.org/10.1016/j.eurpolymj.2023.112291>.
- [221] W. Sheng, B. Li, X. Wang, B. Dai, B. Yu, X. Jia, F. Zhou, Brushing up from “anywhere” under sunlight: a universal surface-initiated polymerization from polydopamine-coated surfaces, *Chem. Sci.* 6 (2015) 2068–2073. <https://doi.org/10.1039/C4SC03851G>.

- [222] F.C.; R.F. Demidoff Eduardo José P.; de Souza, Andréa Luzia F.; Netto, Chaquip D.; de Carvalho, Leandro L., Cross-Coupling Reactions with 2-Amino-/Acetylamino-Substituted 3-Iodo-1,4-naphthoquinones: Convenient Synthesis of Novel Alkenyl- and Alkynyl-naphthoquinones and Derivatives, *Synthesis* 53 (2021) 4097–4109. <https://doi.org/10.1055/s-0037-1610781>.
- [223] K. Narita, N. Fujisaki, Y. Sakuma, T. Katoh, A novel approach to oxazole-containing diterpenoid synthesis from plant roots: salviamines E and F11 Electronic supplementary information (ESI) available: Copies of ¹H and ¹³C NMR spectra for all new compounds. See DOI: 10.1039/c8ob03030h, *Organic & Biomolecular Chemistry* 17 (2019) 655–663. <https://doi.org/10.1039/c8ob03030h>.
- [224] A. Krishnan, S. Kamaraj, Direct Access to Quinone-Fused 5-Substituted-1,4-Benzodiazepine Scaffolds from Azidoquinones with/without [1,2]-Azide-Nitrogen Migration: Mechanistic Insights, *J. Org. Chem.* 88 (2023) 16315–16329. <https://doi.org/10.1021/acs.joc.3c01810>.
- [225] W.S.C. do Nascimento Celso Amorim; de Oliveira, Ronaldo Nascimento, Synthesis of 2-(1H-1,2,3-Triazol-1-yl)-1,4-naphthoquinones from 2-Azido-1,4-naphthoquinone and Terminal Alkynes, *Synthesis* 2011 (2011) 3220–3224. <https://doi.org/10.1055/s-0030-1260172>.
- [226] K. Sun, S. Liu, C. Pigot, D. Brunel, B. Graff, M. Nechab, D. Gignes, F. Morlet-Savary, Y. Zhang, P. Xiao, F. Dumur, J. Lalevé, Novel Push–Pull Dyes Derived from 1H-cyclopenta[b]naphthalene-1,3(2H)-dione as Versatile Photoinitiators for Photopolymerization and Their Related Applications: 3D Printing and Fabrication of Photocomposites, *Catalysts* 10 (2020) 1196. <https://doi.org/10.3390/catal10101196>.
- [227] K. Sun, C. Pigot, Y. Zhang, T. Borjigin, F. Morlet-Savary, B. Graff, M. Nechab, P. Xiao, F. Dumur, J. Lalevé, Sunlight Induced Polymerization Photoinitiated by Novel Push–Pull Dyes: Indane-1,3-Dione, 1H-Cyclopenta[b]Naphthalene-1,3(2H)-Dione and 4-Dimethoxyphenyl-1-Allylidene Derivatives, *Macromolecular Chemistry and Physics* 223 (2022) 2100439. <https://doi.org/10.1002/macp.202100439>.